

PART 4 – TRANSMITTING AND RECEIVING APERTURES

Section	Page
Radio Frequency Antennas	234
Optical Frequency Apertures	282
Optical Apertures – Optical Configurations	296
Optical Frequency Apertures – Weight and Cost Relationships	318

INTRODUCTION

Antenna theory and state-of-the art are related to weight and cost of the antennas in the subsequent sections.

This section presents the theory and state of the art of radio frequency antennas potentially capable of fulfilling the characteristics dictated by space communication and tracking applications.

Antenna Theory for Large Apertures is discussed first. The fundamental parameters for characterizing antenna performance are defined. In addition, an analysis relating the degradation of performance to phase errors caused by both bending and random distortion of large antennas is given.

The Antennas for Space Communication Section describes antenna types potentially suitable for space communication and tracking applications. Also indicated is the performance and relative advantages of the various antenna types for different space applications. Curves showing degradation of antenna gain as a function of aperture distortion for various types of antennas are given.

The radio frequency antenna discussion is concluded by giving antenna burden relationships. Included are cost and weight relationships.

SUMMARY OF RF TRANSMITTING AND RECEIVING APERTURES

Phased array and parabolic dish transmitting and receiving antennas are the most useful antenna types for deep space missions.

High gain antennas may be designed as arrays of low or moderate gain elements, or as large area reflector surfaces illuminated by moderate gain feed elements. Array elements, for the operating frequencies of interest for space communication, are in general heavier than a reflector antenna of the same gain. This is attributable to need for relatively complex radiating element structures as contrasted to a simple reflector surface, and to the requirement for a complex feed system for the array antenna as contrasted to free space for the reflector antenna. Conversely array antennas have an inherent capability for forming multiple beams which may be switched rapidly from one beam to another with no moving parts. These characteristics overpower weight considerations and lead to their selection for specialized communication missions. The reflector antenna is, however, considered suitable for specific area coverage broadcast satellites and for wide bandwidth data links for planetary and deep space probes.

Two types of directive antennas are most commonly used for space communications. These are the parabolic dish and the planar array antenna.

Reflector-Type Antenna. This antenna has two basic components: a relatively large reflecting surface (most often paraboloidal) and a feed structure. When maximum antenna gain is required, as for space communication and tracking, the reflector size is chosen to be as large as practical and the feed is normally designed to illuminate the reflector with an intensity at the reflector edges that is approximately 10 db below that at the center.

The efficiencies of reflector-type antennas with a front-mounted feed are typically 55 percent, with 65 percent being the upper realizable bound. The efficiencies of cassegrainian type antennas are typically 60 percent with 70 percent being the upper realizable bound.

The figure illustrates the performance of several large ground based antennas as a function of wavelength, as documented by Ruze.¹

In addition to earth antennas, parabolic antennas have been used on the Pioneer spacecraft and the Mariner spacecraft.

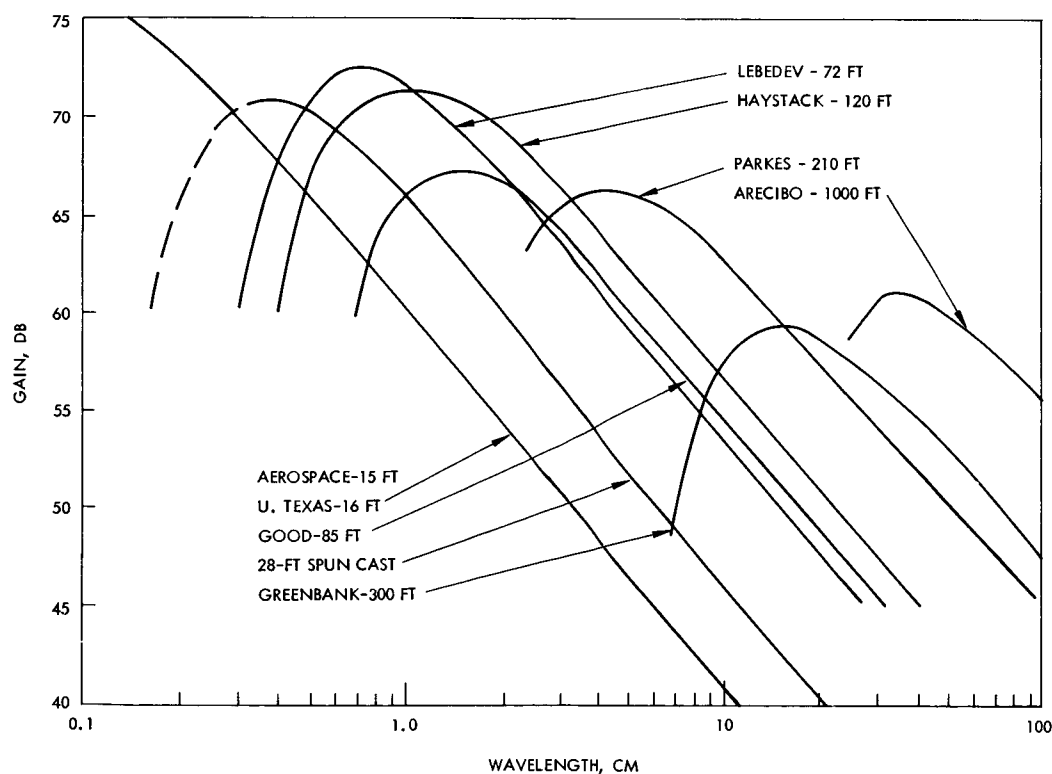
Phased Array Antenna. This type of antenna consists of an array of radiating elements with either fixed or variable relative phase differences. Those with fixed relative phase differences are referred to as planar

¹ Ruze, J., "Antenna Tolerance Theory - A Review, " Proc. IEEE, pp. 633-640, April 1966.

arrays and require mechanical pointing. Those with variable relative phase differences require external electronic controls to properly phase the elements to form a beam in a desired direction. When maximum antenna gain is required, as for space communication and tracking, all the elements of the array are excited equally and the relative phase between elements is adjusted for a beam normal to the plane of the array.

The weight, complexity, and cost of the variable phase shifters needed for those antennas with variable phase differences have deterred space applications of electronically scanned phased arrays. Planar arrays have been used on the ground and even in space when the type of space vehicle stabilization permitted mechanical beam steering.

A planar array antenna was used on the Surveyor spacecraft. This antenna measured 38 x 38 x 2 inches and had a gain of 27 db at 2300 MHz. Planar arrays have advantages of higher efficiency and lower volume than parabolic antennas of equivalent gain. Their chief disadvantage is higher cost.



Gain of Large Paraboloids

TRANSMITTING AND RECEIVING APERTURES RADIO FREQUENCY ANTENNAS

Antenna Theory for Large Antennas Apertures

Antenna Gain and Aperture Relationships	Page 240
Gain Degradation Due to Predictable Systematic (Non-Random) Phase Errors	244
Gain Degradation Due to Random Errors	248
Effects of Random Errors on Antenna Parameter Values	252

ANTENNA GAIN AND APERTURE RELATIONSHIPS

Relationships of antenna gain, aperture, and aperture energy distribution are given.

A microwave antenna is a transducer between electromagnetic waves contained by a transmission line and those radiated through space. The spatial distribution of the radiated electromagnetic waves in terms of intensity of energy flow is called the antenna pattern. More precisely, the antenna pattern in a specified plane is a plot of the power radiated per unit solid angle versus a space coordinate, which is usually an angle. Antennas in general are reciprocal and therefore the spatial antenna patterns are independent of whether the antenna is radiating into or receiving from space.

For a fixed frequency; beamwidth, gain, effective area, and sidelobe level are the parameters which are most important in characterizing the performance of antennas. The beamwidth is defined as the angular width at the half power or 3 db points of the main beam of the antenna pattern. The half power points on the main beam are those points where the power received or transmitted is one-half of the value at the beam peak. The portions of the antenna pattern, other than the main beam, are called sidelobes. The sidelobe level, usually quoted in decibels, is the ratio of the maximum power density in the largest sidelobe (usually the sidelobe adjacent to the main beam) to the power density in the main beam maximum. Sidelobes play an important part of determining antenna system noise temperatures, especially for high sensitivity earth antennas.

The antenna gain, G , expresses the ability of an antenna to concentrate the radiated power in a particular direction or, conversely, to absorb power incident from a particular direction more effectively than from other directions. G is defined as the ratio of power per unit solid angle in the direction of the peak of the main beam to the average radiated per unit solid angle. Let P_M be the power radiated per unit solid angle in the direction of the peak of the main beam and let P_t be the total power radiated when the antenna is perfectly matched.

Then

$$G = \frac{P_M}{P_t/4\pi}$$

Another measure of receiving antenna performance is effective area, or receiving cross section. Effective area is the area of a perfect antenna which absorbs the same amount of power from an incident plane wave as the actual antenna. Gain and effective area A_E are simply related as

$$\frac{G}{A_E} = \frac{4\pi}{\lambda^2}$$

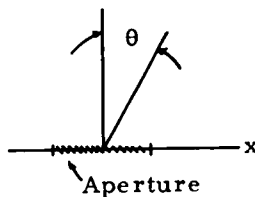
Let G_T and G_R be the respective antenna gains of a transmitting antenna and a receiving antenna separated by a distance R . If the total power transmitted is P_T , the power radiated in the direction of the main beam aimed at the receiver, per unit solid angle will be $P_T G_T / 4\pi$. The receiving antenna will present a receiving cross section $G_R \lambda^2 / 4\pi$ to the incident wave; it will, in effect, subtend a solid angle $G_R \lambda^2 / 4\pi R^2$ at the transmitter. The power absorbed at the receiver will thus be

$$P_R = P_T \frac{G_T G_R \lambda^2}{16\pi^2 R^2}$$

Here it is seen that the power received in space communication is directly related to the power transmitted as well as to the gain of both the receiving and transmitting antennas. Hence, for efficient transmission the gain of both the relatively small spacecraft antenna and the gain of the large ground station antenna have to be maximized within practical limitations. The most evident practical limitation on the gain of spacecraft antennas is the size allowed by the shroud of the launch vehicles. However, inflatable or unfurlable spacecraft antennas are exceptions to this size limitation. The gain associated with all antennas is dependent on the ability to maintain the desired amplitude and phase of the antenna's aperture illumination.

The spatial antenna pattern is $|g(y)|^2$, where $y = \sin \theta$, and is related to the aperture distribution $f(x)$ by:

$$g(u) = \int_a f(x) e^{jkyx} dx, \quad K = \frac{2\pi}{\lambda}$$



where a is the aperture. If the aperture consists of discrete sources, the above integration degenerates into a summation. Some typical, but common aperture distributions and their associated antenna patterns are given in Table 1¹. The following general observations may be made:

1. A uniform amplitude distribution provides highest gain (constant phase cases).

¹ Silver, S., Microwave Antenna Theory and Design, 12, Rad. Lab Series, McGraw Hill.

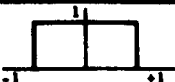



ANTENNA GAIN AND APERTURE RELATIONSHIPS

2. Tapering the amplitude from a high value near the center to a low value near the edges reduces the sidelobe level, increases the beamwidth, and decreases the gain from the uniformly illuminated case.
3. Tapering the amplitude from a low value near the center to a high value near the edges reduces the beamwidth, increases the sidelobe level, and decreases the gain from the uniformly illuminated case.

Relations among the various antenna parameters for many popular, specific cases are given in Figures A² and B².

²ITE Antenna Handbook.

Table 1. Secondary Pattern Characteristics Produced by Various Types of Aperture Distributions

 $f(x) = 1 \quad x \leq 1$ $= 0 \quad x > 1$ $g(u) = \frac{\sin u}{u}$				
	Gain factor \mathcal{A}_n ‡	Full width at half power Θ , radians	Angular position θ of first zero	Intensity of first side lobe: db below peak intensity
	1	$0.88 \frac{\lambda}{a}$	$\frac{\lambda}{a}$	13.2
 $f(x) = 1 - (1 - \Delta)x^2, x < 1$ $= 0 \quad x > 1$ $g(u) = a \left[\frac{\sin u}{u} + (1 - \Delta) \frac{d^2}{du^2} \left(\frac{\sin u}{u} \right) \right]$ $\mathcal{A}(\Delta) = \frac{(2 + \Delta)^2}{9 \left[1 - \frac{2}{3}(1 - \Delta) + \frac{1}{3}(1 - \Delta)^2 \right]}$				
$\Delta = 1.0$	1	$0.88 \frac{\lambda}{a}$	$\frac{\lambda}{a}$	13.2
0.8	0.994	$0.92 \frac{\lambda}{a}$	$1.06 \frac{\lambda}{a}$	15.8
0.5	0.970	$0.97 \frac{\lambda}{a}$	$1.14 \frac{\lambda}{a}$	17.1
0.0	0.833	$1.15 \frac{\lambda}{a}$	$1.43 \frac{\lambda}{a}$	20.6
 $f(x) = \cos^n \frac{\pi x}{2}, x < 1$ $= 0 \quad x > 1$ $g(u) = \frac{2a}{\pi} \frac{n! \cos u}{\sum_{k=0}^{\frac{n-1}{2}} \left[(2k+1)^2 - \frac{4u^2}{\pi^2} \right]}$ n , odd; $g(u) = a \frac{n!}{\sum_{k=1}^{\frac{n}{2}} \left[(2k)^2 - \frac{4u^2}{\pi^2} \right]} \cdot \frac{\sin u}{u}$ n , even $\mathcal{A}_n = \frac{4}{\pi^2} \left[\frac{2 \cdot 4 \cdot 6 \cdots (n-1)}{1 \cdot 3 \cdot 5 \cdots n} \right]^2$ $\left(\frac{2 \cdot 4 \cdot 6 \cdots 2n}{1 \cdot 3 \cdot 5 \cdots 2n-1} \right) n$, odd $\mathcal{A}_n = \left[\frac{1 \cdot 3 \cdot 5 \cdots (n-1)}{2 \cdot 4 \cdot 6 \cdots n} \right]$ $\left[\frac{(n+2)(n+4) \cdots 2n}{(n+1)(n+3) \cdots 2n-1} \right] n$, even				
$n = 0$	1	$0.88 \frac{\lambda}{a}$	$\frac{\lambda}{a}$	13.2
1	0.810	$1.2 \frac{\lambda}{a}$	$1.5 \frac{\lambda}{a}$	23
2	0.667	$1.45 \frac{\lambda}{a}$	$2 \frac{\lambda}{a}$	32
3	0.575	$1.66 \frac{\lambda}{a}$	$2.5 \frac{\lambda}{a}$	40
4	0.515	$1.93 \frac{\lambda}{a}$	$3 \frac{\lambda}{a}$	48
 $f(x) = 1 - x , x < 1$ $= 0 \quad x > 1$ $g(u) = 4a \left(\frac{\sin \frac{u}{2}}{\frac{u}{2}} \right)^2$				
	0.75	$1.28 \frac{\lambda}{a}$	$2 \frac{\lambda}{a}$	26.4
<p>* $u = \frac{\pi a}{\lambda} \sin \theta$</p> <p>‡ a = aperture length</p> <p>§ The efficiency of the aperture in concentrating the available energy into the peak intensity of the beam. Values are less than unity.</p>				

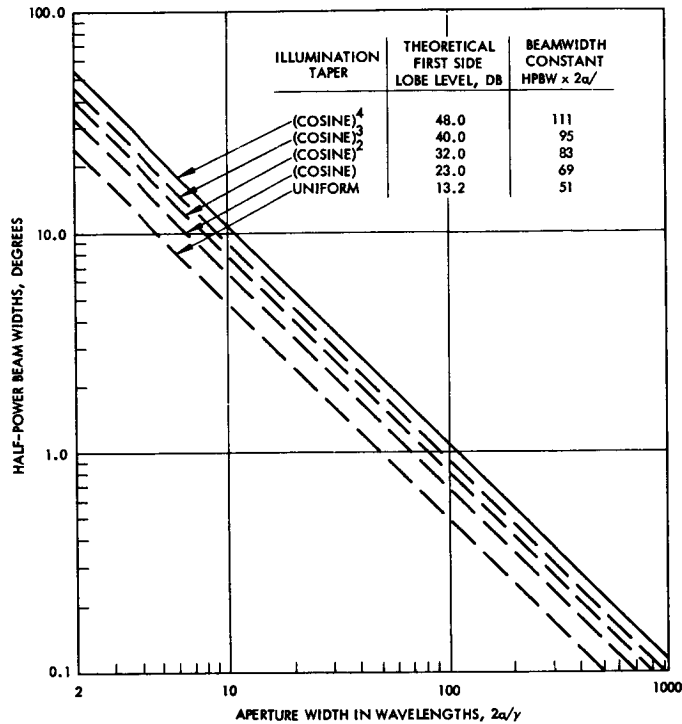


Figure A. Antenna Half-Power Beamwidths Versus Aperture Widths for Rectangular Apertures

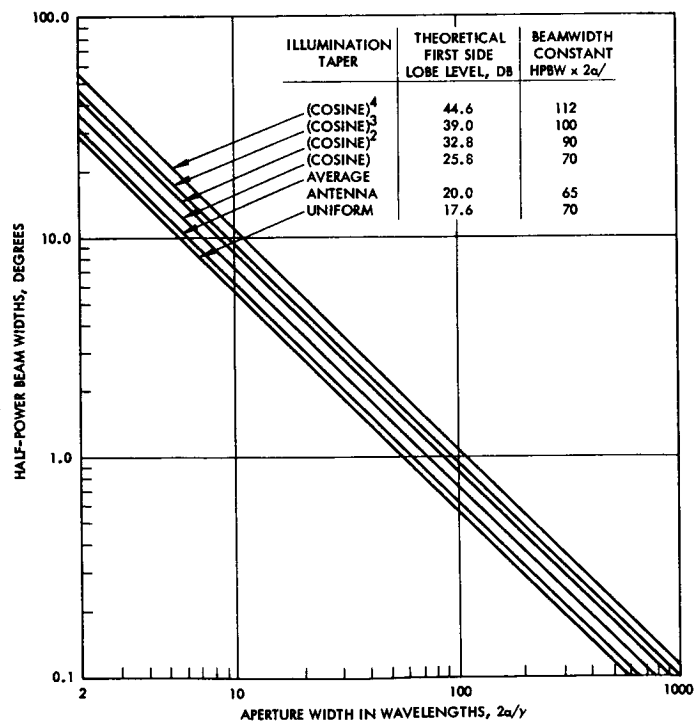


Figure B. Antenna Half-Power Beamwidths Versus Aperture Width for Circular or Elliptical Apertures

GAIN DEGRADATION DUE TO PREDICTABLE SYSTEMATIC (NON RANDOM) PHASE ERRORS

Maximum antenna gain degradation due to "worst case" distortion is calculated and plotted.

Bailin¹ has investigated the effect of array bending on the far field radiation pattern of a large linear array of closely spaced elements. The particular type of bending which was shown to produce the severest gain degradation is the bending of an array supported at one fourth the array length from each end as shown in Figure A. The far field radiation pattern of such a bent array was shown to be proportional to

$$g(W, B) \sim \frac{\sin W\pi/2}{W\pi/2} \left[1 - \frac{B^2}{(2^2 - W^2)} \left(1 - \frac{W^2}{2!} \right) + \frac{B^4}{(2^2 - W^2)(4^2 - W^2)} \left(1 - \frac{W^2}{2!} + \frac{W^2(2^2 - W^2)}{4!} \right) + \dots \right] - j \frac{2W}{\pi} \cos \frac{W\pi}{2} \left[\frac{B}{1 - W^2} - \frac{B^3}{(1 - W^2)(3^2 - W^2)} \left(1 - \frac{1 - W^2}{3!} \right) + \frac{B^5 + (1 - W^2)/3! + (1 - W^2)(3^2 - W^2)/5!}{(1 - W^2)(3^2 - W^2)(5^2 - W^2)} + \dots \right] \quad (1)$$

where

$$W = \frac{kc}{\pi} \sin \theta \quad (= 0 \text{ at } \theta = 0^\circ)$$

and

$$B = kB_0 \cos \theta = \frac{2\pi}{\lambda} \frac{\lambda}{N} \cos \theta \quad (= \frac{2\pi}{N} \text{ at } \theta = 0^\circ)$$

B_0 = the maximum amplitude of the phase distortion measured in radians as a fraction of a wavelength, λ/N

$$K = \frac{2\pi}{\lambda}$$

N is an integer

¹Bailin, L. L., "Fundamental Limitations of Long Arrays," Hughes Aircraft Company, Technical Memorandum TM330, October 1953.

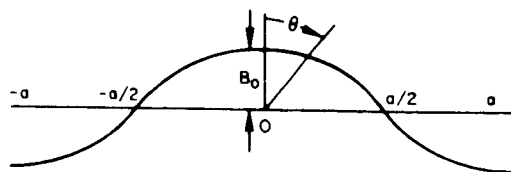


Figure A. Bending of an Array
Supported at One Fourth the
Array Length From Each
End

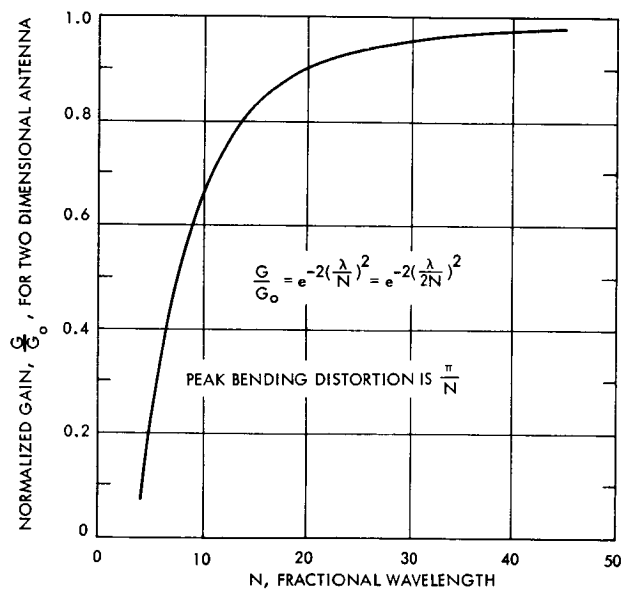


Figure B. Gain Loss in a Two Dimensional
Antenna Due to Non-Random Bending

GAIN DEGRADATION DUE TO PREDICTABLE SYSTEMATIC (NON RANDOM) PHASE ERRORS

In order to simplify the derivation, the gain degradation in this non random phase error portion of the analysis will be calculated as the reduction of P_M , the power radiated per solid angle in the direction of the peak of the main beam ($\theta = 0^\circ$). This equality is only approximate since P_t , the total power radiated, can also vary as a function of phase distortion. With this approximation the gain degradation of the linear array can readily be obtained by the square of the far field radiation pattern, Equation (1), evaluated at $\theta = 0^\circ$.

$$\frac{G}{G_{Lo}} = \left[1 - \frac{B^2}{4} \right]^2 \quad (2)$$

$$= \left[1 - \left(\frac{\pi}{N} \right)^2 \right]^2 \quad (3)$$

$$= e^{-2(\pi/N)^2} \quad (4)$$

for small values of (π/n)

where G_L is the gain of a one-dimensional antenna and G_{Lo} is the no-error gain of the same antenna.

Squaring Equation 4 results in the gain degradation of a two-dimensional antenna.

$$\frac{G}{G_o} = e^{-4(\pi/N)^2} \quad (5)$$

where G is the gain of a two-dimensional antenna, and G_o is the no-error gain of a two-dimensional antenna. This relationship is plotted in Figure B. Figure C is a plot of the db loss for two types of bending distortion analyzed by Bailin. Figure D relates this distortion to antenna gain.

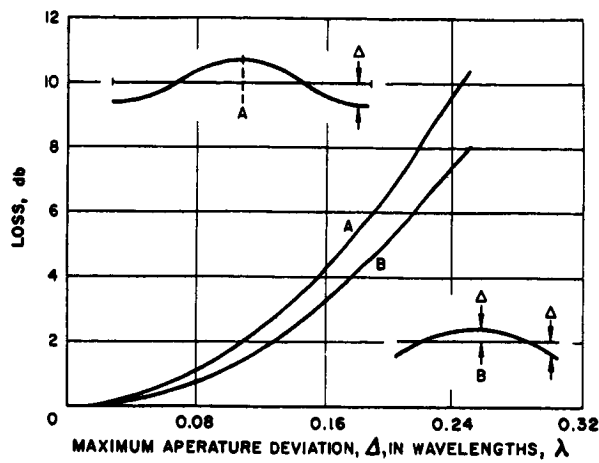


Figure C. Degradation in Gain Due to Sinusoidal Deflection of Paraboloid

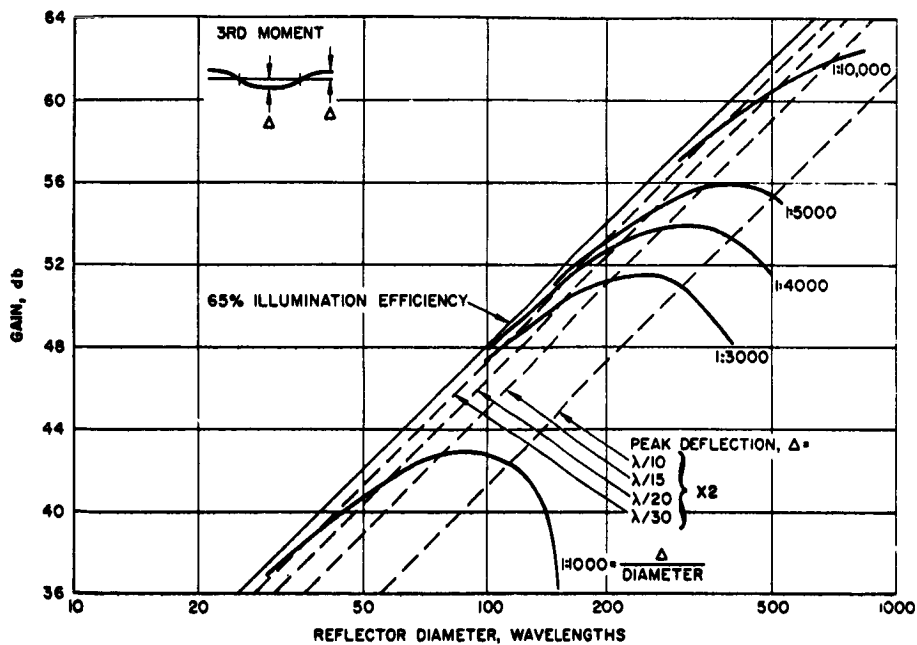


Figure D. Gain versus Reflector Distortion

GAIN DEGRADATION DUE TO RANDOM ERRORS

Random phase errors produce a degradation which are the square root of degradation produced by non-random errors.

Ruze¹ has statistically analyzed the degradation of two-dimensional antenna gain due to random phase errors. The phase errors of concern here are those random phase errors caused by loose machining tolerances and random distortion of the aperture surface. Ruze considered both discrete array and continuous aperture antennas. In general the same statistical considerations apply to the continuous aperture antenna as to the discrete array antenna. In the discrete array case, the error in one array element is independent of the errors in adjacent elements. However, this assumption is untenable in an aperture antenna since if the error is large at one point it will probably be large in its immediate neighborhood. Therefore a "correlation interval," C , is defined as that distance "on average" where the errors become essentially independent.

For small correlation intervals $C/\lambda \ll 1$

$$\frac{G}{G_0} \approx 1 - \frac{3}{4} \overline{\delta^2} \frac{C^2 \pi^2}{\lambda^2} \quad (1)$$

$$\approx \exp \left[-\frac{3}{4} \overline{\delta^2} \frac{C^2 \pi^2}{\lambda^2} \right] \text{ for small values of } \frac{3}{4} \overline{\delta^2} \frac{C^2 \pi^2}{\lambda^2} \quad (2)$$

where $\overline{\delta^2}$ is the mean square phase deviation in radians.

For large correlation intervals

$$\frac{G}{G_0} \approx 1 - \overline{\delta^2} \quad (3)$$

$$\approx e^{-\overline{\delta^2}} \text{ for small values of } \overline{\delta^2} \quad (4)$$

With equations describing the gain degradation of two-dimensional antennas due to random phase errors and another describing the gain degradation due to non random phase errors caused by array bending, * it would be of interest to compare the gain degradation predicted by the

¹Ruze, J., "The Effect of Aperture Errors on the Antenna Radiation Pattern," Supplemento AL Volume IX, Serie IX Del Nuovo Cimento No. 3, 1952.

*See previous topic.

two different analyses for identical rms phase errors. For convenience, the gain degradation is calculated for non random phase errors caused by bending the array supported at one fourth the array length from each end as shown in Figure A of the previous topic. This value of gain degradation is to be compared with that introduced by a random phase error of identical rms value, for the same two-dimensional antenna.

For a $2\pi/N$ value of maximum amplitude of phase distortion, the mean square phase degradation, $\overline{\delta^2}$, in radians can be determined as follows along the path " ℓ " for an aperture size " a " to be

$$\overline{\delta^2} = \frac{1}{a} \int_{-a/2}^{a/2} f^2(\ell) d\ell \quad (5)$$

$$\overline{\delta^2} = \frac{1}{a} \int_{-a/2}^{a/2} \left(\frac{2\pi}{N}\right)^2 \cos^2\left(\frac{2\pi}{a}\ell\right) d\ell \quad (6)$$

$$\overline{\delta^2} = \frac{1}{a} \left(\frac{2\pi}{N}\right)^2 \left[\left(\frac{\cos(2\pi\ell/a)}{4(2\pi/a)^2} \right) \left(2 \frac{2\pi}{a} \sin \frac{2\pi\ell}{a} \right) + \frac{2(2\pi/a)^2}{4(2\pi/a)^2} \ell \right] \Bigg|_{-\frac{a}{2}}^{\frac{a}{2}} \quad (7)$$

$$\overline{\delta^2} = 2 \left(\frac{\pi}{N}\right)^2 \quad (8)$$

Substituting Equation (8) into Equations (3) and (4) yields a gain degradation for random errors of:

$$\frac{G}{G_o} \approx 1 - 2 \left(\frac{\pi}{N}\right)^2 \quad (9)$$

or for small values of π/N

$$\frac{G}{G_o} \approx e^{-2(\pi/N)^2} \quad (10)$$

This is plotted in Figure A.

GAIN DEGRADATION DUE TO RANDOM ERRORS

Random phase error Equation (4) predicts a gain degradation which is the square root of the gain degradation predicted by non random phase error for the same rms phase errors. This result can be explained heuristically as follows. In the non random case, waves from relatively large portions of the aperture are in phase and of different phase than waves from other relatively large portions of the aperture. The two groups of waves destructively interfere with each other much more effectively than groups consisting of waves with random phase even though the mean square phase deviation is the same in both cases.

Antenna gain degradation is due to two distinct types of aperture distortion, random and non random. Curves depicting antenna gain as a function of aperture size in wavelengths for various amounts of random aperture phase distortion are presented in the next topic.

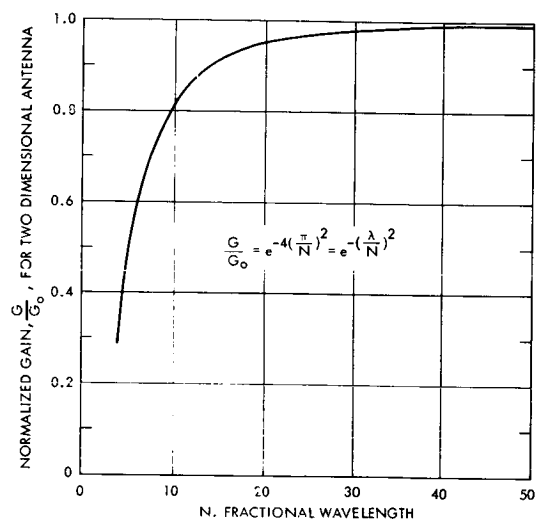


Figure A. Gain Loss in a Two Dimensional Antenna Due to Random Errors

EFFECTS OF RANDOM ERRORS ON ANTENNA PARAMETER VALUES

Curves are presented in this topic which depict antenna gain as a function of aperture size in wavelengths for various amounts of random aperture phase distortion and for various types of antennas.

The efficiency of an antenna is the ratio of its effective area A_E to its actual area A_A .

$$\text{Eff} = \frac{A_E}{A_A} \quad (1)$$

Recalling that

$$\frac{G}{A_E} = \frac{4\pi}{\lambda^2} \quad (2)$$

allows the gain to be written as

$$G = \frac{4\pi \text{Eff} A_A}{\lambda^2} \quad (3)$$

Efficiencies of reflector type antennas range from 55 to 70 percent and efficiencies of planar arrays range from 70 to 85 percent. Efficiencies of horn radiators range from 85 to 95 percent. For convenience it is assumed circular apertures of area $\pi D^2/4$, where D is the diameter.

For a circular aperture antenna with uniform phase and amplitude aperture illumination the gain may be expressed as

$$G = \frac{4\pi \text{Eff}}{\lambda^2} \left(\frac{\pi D^2}{4} \right) = \text{Eff} \left(\frac{\pi D}{\lambda} \right)^2 \quad (4)$$

Figures A, B, and C present the error-free antenna gain and gain with random phase errors as a function of aperture size in wavelengths. The root mean square phase error in each figure is a particular fraction of the electrical diameter in radians. Therefore, the rms phase error on one curve is greater for the large diameter circular planar arrays and parabolic reflectors. The random phase error curves are valid only for small rms values of phase error.

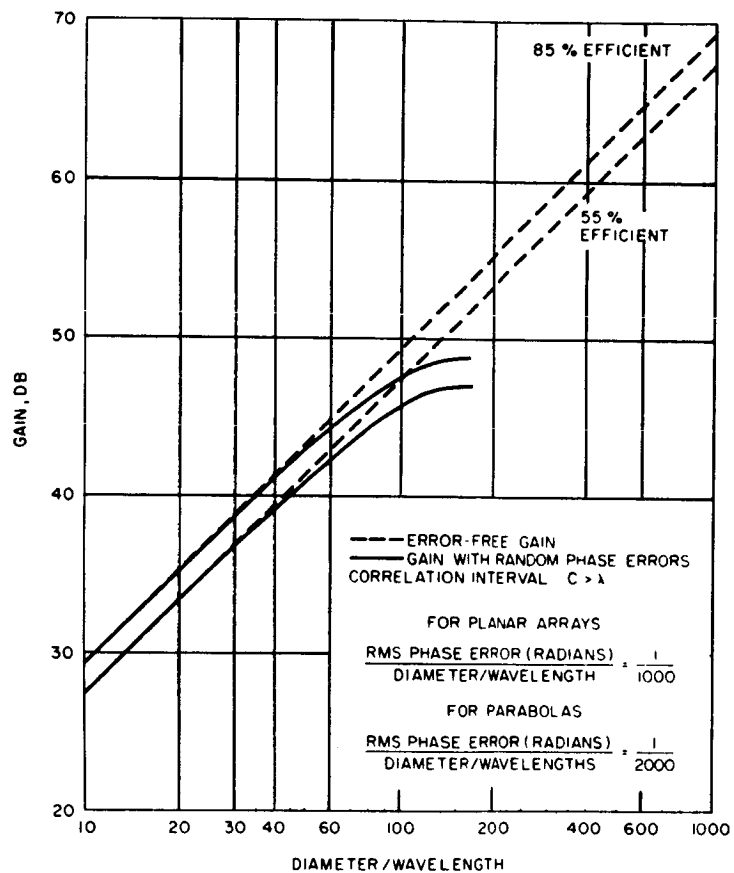


Figure A. Antenna Gain Degradation Due to Random Phase Errors in Aperture Illumination

EFFECTS OF RANDOM ERRORS ON ANTENNA PARAMETER VALUES

Figure D¹ presents the loss of gain due to reflector tolerance as a function of frequency.

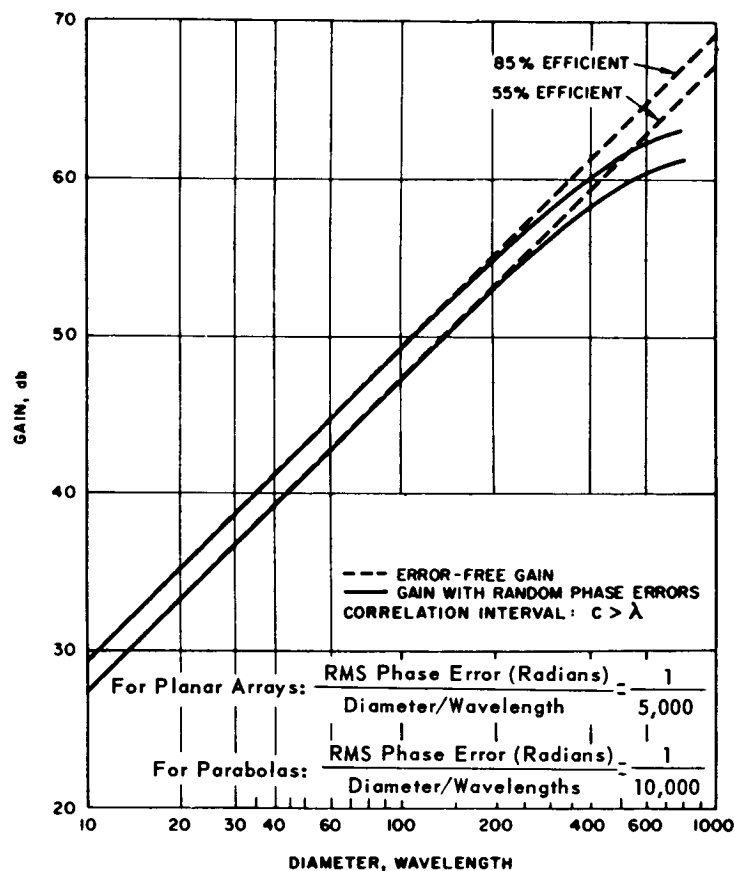


Figure B. Antenna Gain Degradation Due to Random Phase Errors in Aperture Illumination

¹ Ruze, J., "Antenna Tolerance Theory - A Review Proc.", IEEE, pp 633-640, April 1966.

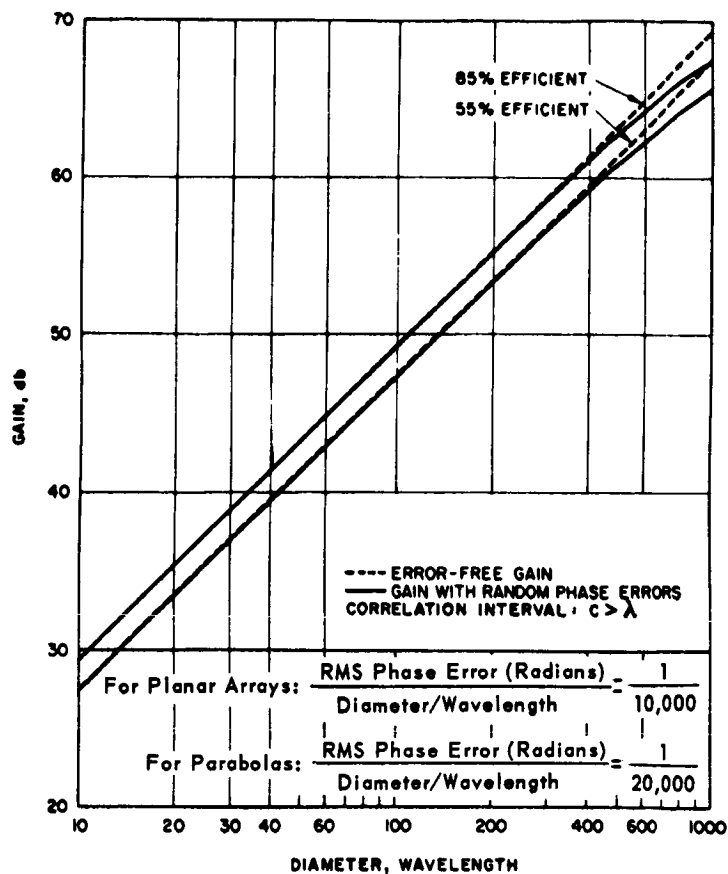
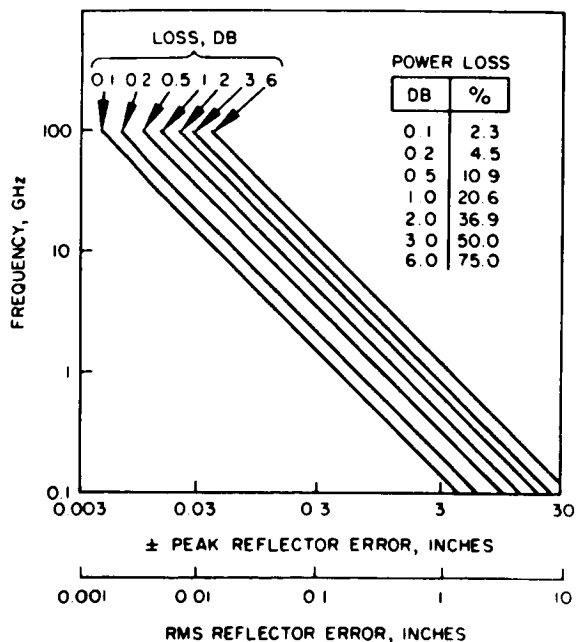


Figure C. Antenna Gain Degradation Due to Random Phase Errors in Aperture Illumination

Figure D. Gain Loss Due to Reflector Tolerance



TRANSMITTING AND RECEIVING APERTURES

Radio Frequency Antennas

	Page
Antennas for Space Communication — Design Considerations	258
Antennas for Space Communication — Antenna Types	260
Antennas for Space Communication — Deployable Paraboloids	262
Antennas for Space Communication — Weight Burdens for Paraboloids	264
Special Purpose Multibeam and Self Steering Antennas	266
High Gain, Self-Steering Antenna System for Satellite-Earth Communications	268
Antennas for Space Communication — Surface Station Cost Burdens	274
Antennas for Space Communication — Spacecraft Cost Burdens	276

ANTENNAS FOR SPACE COMMUNICATION — DESIGN CONSIDERATIONS

High gain antennas are considered for ranges greater than synchronous orbit.

Antenna design is limited by considerations of beamwidth, frequency, launch vehicle payload weight limits, and restrictions on payload package dimensions during boost. It seems reasonable to restrict consideration of high gain spacecraft antenna to satellites in synchronous earth orbits and to deep space and planetary probes. Low altitude satellites require wide angle coverage for effective coverage, and as the range is not too great, moderate transmitter levels are adequate for communication with the earth. Synchronous altitude satellites require an antenna with a beamwidth of 20 degrees to provide for earth coverage and to allow for spacecraft attitude errors. A lower limit of 0.7 degree is suggested from the standpoint of spacecraft attitude control.¹ If the antenna beam is nominally centered on the receiving station, a variation of spacecraft attitude by ± 0.1 degree will result in power level variations of approximately 1 db. Finer control may perhaps be accomplished but only at the expense of added complexity of the control system.

Booster payload weight and size limitations are important design limits for the spacecraft and its subsystems. Allowable weight bogies for spacecraft antenna subsystems cover many orders of magnitude for the currently available and projected launch vehicles. Satellite payloads approximately 9 feet in diameter can be accommodated by currently available launch vehicles without resorting to deployment mechanisms.

¹ Patton, W. T. and Glenn, A. B., "Component Problems in a Microwave Deep Space Communication System," Conference Record, WINCON, Los Angeles, Calif., 1966.

ANTENNAS FOR SPACE COMMUNICATION — ANTENNA TYPES

Phased array antennas are compared with parabolic dish antennas. The latter is the subject of subsequent topics.

High gain antennas may be designed as arrays of low or moderate gain elements, or as large area reflector surfaces illuminated by moderate gain feed elements. Array elements, for the operating frequencies of interest for space communication, are in general heavier than a reflector antenna of the same gain. This is attributable to need for relatively complex radiating element structures as contrasted to a simple reflector surface, and to the requirement for a complex feed system for the array antenna as contrasted to free space for the reflector antenna. Array antennas have an inherent capability for forming multiple beams which may be switched rapidly from one beam to another with no moving parts. These characteristics overpower weight considerations and lead to their selection for specialized communication missions. The reflector antenna is, however, considered suitable for specific area coverage broadcast satellites and for wide bandwidth data links for planetary and deep space probes.

Examination of world geography shows that pencil beams are desirable to conserve radiated power by directing it toward the areas of interest. North America, Europe, Africa or the whole earth can be effectively covered by circular pencil beams. Paraboloid antennas can be designed with primary focus feed or with secondary reflector feeds. The primary reflector structural design approach affects weight to a larger degree than does the feed. It is, therefore, proposed to classify antenna designs by means of their structural design approaches.

Two types of directive antennas are most commonly used for space communications. These are the parabolic dish and the planar array antenna. Some performance characteristics for these antennas has been given in prior topics. Further data are given in this topic with brief comments on construction of these two types of antennas.

Reflector-Type Antenna. This antenna has two basic components: a relatively large reflecting surface (most often paraboloidal) and a feed structure. When maximum antenna gain is required, as for space communication and tracking, the reflector size is chosen to be as large as practical and the feed is normally designed to illuminate the reflector with an intensity at the reflector edges that is approximately 10 db below that at the center.

The efficiencies of reflector-type antennas with a front-mounted feed are typically 55 percent, with 65 percent being the upper realizable bound. The efficiencies of cassegrainian type antennas are typically 60 percent with 70 percent being the upper realizable bound.

The figure illustrates the performance of several large ground based antennas as a function of wavelength, as documented by Ruze.¹

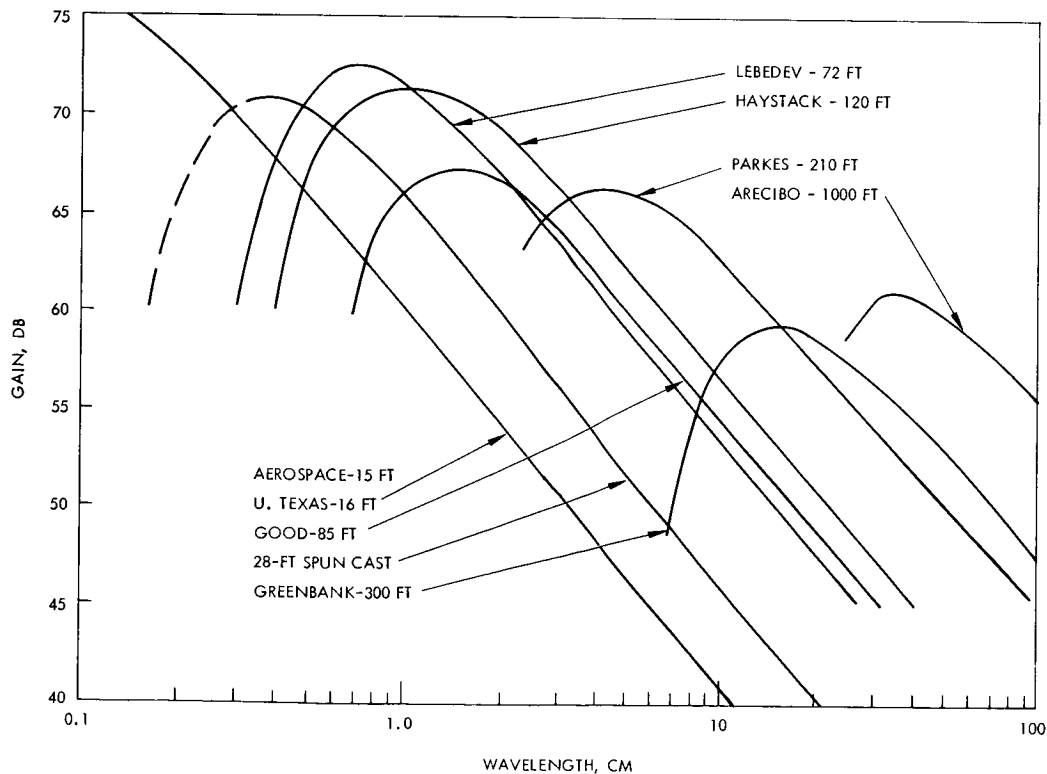
¹Ruze, J., "Antenna Tolerance Theory — A Review," Proc. IEEE, pp. 633-640, April 1966.

In addition to earth antennas, parabolic antennas have been used on the Pioneer spacecraft and the Mariner spacecraft.

Phased Array Antenna. This type of antenna consists of an array of radiating elements with either fixed or variable relative phase differences. Those with fixed relative phase differences are referred to as planar arrays and require mechanical pointing. Those with variable relative phase differences require external electronic controls to properly phase the elements to form a beam in a desired direction. When maximum antenna gain is required, as for space communication and tracking, all the elements of the array are excited equally and the relative phase between elements is adjusted for a beam normal to the plane of the array.

The weight, complexity, and cost of the variable phase shifters needed for those antennas with variable phase differences have deterred space applications of electronically scanned phased arrays. Planar arrays have been used on the ground and even in space when the type of space vehicle stabilization permitted mechanical beam steering.

A planar array antenna was used on the Surveyor spacecraft. This antenna measured 38 x 38 x 2 inches and had a gain of 27 db at 2300 MHz. Planar arrays have advantages of higher efficiency and lower volume than parabolic antennas of equivalent gain. Their chief disadvantage is higher cost.



Gain of Large Ground Based Paraboloids

ANTENNAS FOR SPACE COMMUNICATION — DEPLOYABLE PARABOLOIDS

Three types of extensible (deployed) spacecraft antennas are discussed: umbrella antenna, inflatable antenna, and petaline antenna.

Qualities of importance for a paraboloid reflector surface are r-f reflectivity, construction accuracy, and low weight. These qualities are closely associated with the type of reflector surfaces material used. Reflectivity can be obtained by thin metalized films, knitted metalized fabric meshes, wire meshes, or solid metallic panels. Aluminum mylar sandwich materials are representative of film materials. Knitted metalized nylon reflective meshes have been developed for radar targets. Similar materials using fused quartz appear ideal for long lifetime applications.

Design approaches may be classified according to the deployment technique used. A technique for deploying metalized film or mesh over a framework of radial ribs forms one class of antenna designs. This general class is illustrated by the design sketch of Figure A. For this design, normally straight ribs are deflected by alignment cables into a parabolic shape. The reflector material is supported by the deflected ribs. This general design approach is called the umbrella type design.

Inflatable structures form a second design classification. As the inflatable will escape in time, these structures must be designed to remain in the deployed configuration following loss of the inflatable. This may be accomplished by utilizing rigidizable materials or by deploying a rigid frame initially. Figures B and C show design sketches of this type of antenna structure. This design approach is generally termed the inflatable type design.

Mechanical deployment of rigid panels is a technique modeled after large ground antennas. Deployment can be accomplished by rotating the individual panels into their position in the paraboloid as illustrated by Figure D. This design approach is termed the petaline type design.

The foregoing design approaches are representative of antenna design approaches in terms of weight and accuracy. Deployment techniques and materials are key areas for advanced design and development. Performance and weight comparisons of the three types are presented in the next topic to develop design comparisons and to show general areas of applicability.

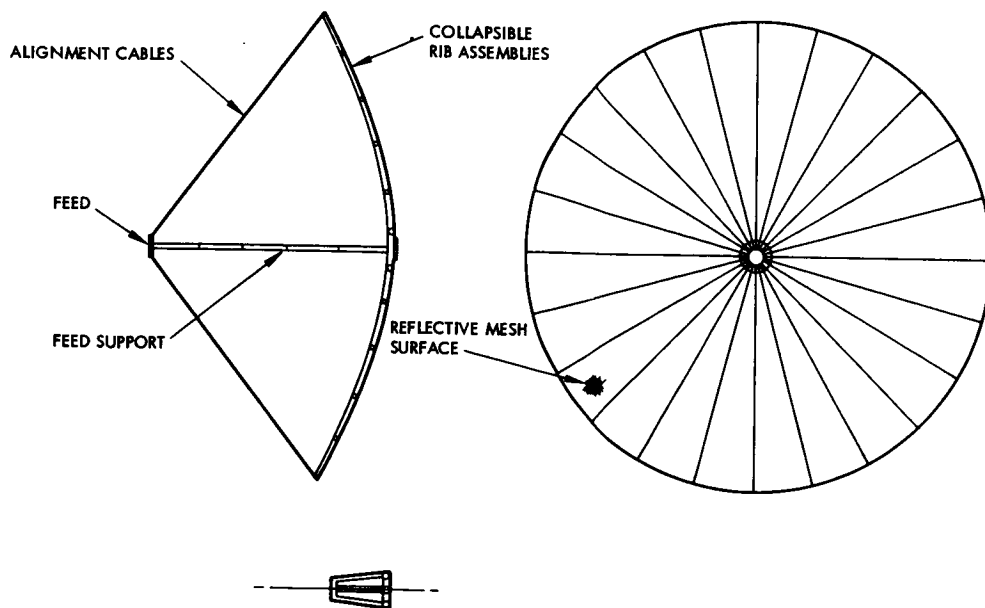


Figure A. Umbrella Antenna Design Concept

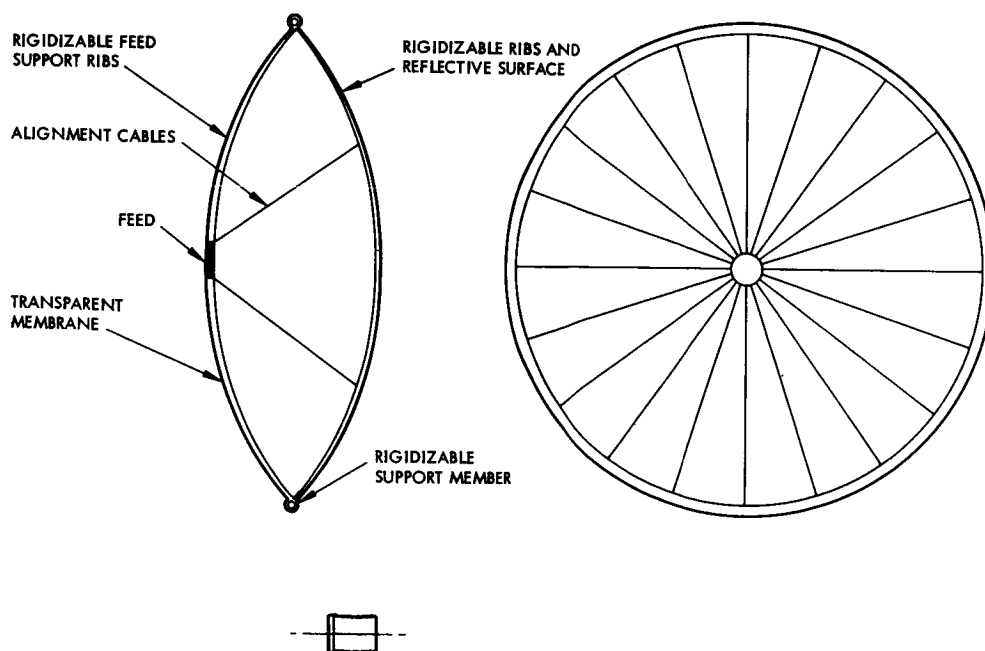


Figure B. Inflatable Antenna Design Concept Rigidizable Ribs and Reflector Surface

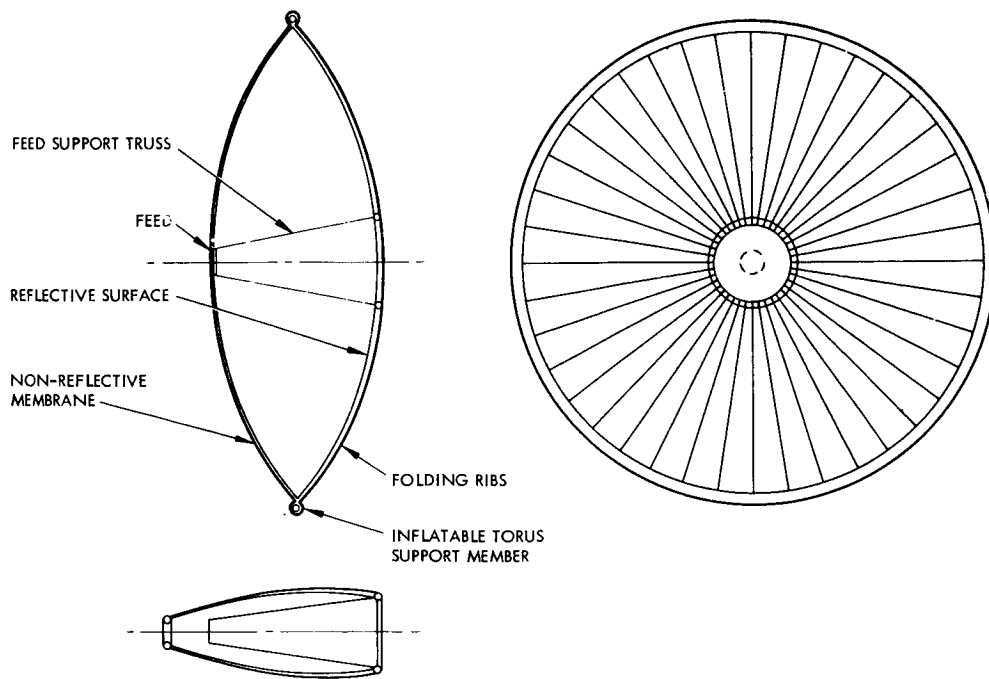


Figure C. Inflatable Antenna Design Concept Rigid Ribs, Rigidizable Reflector Surface

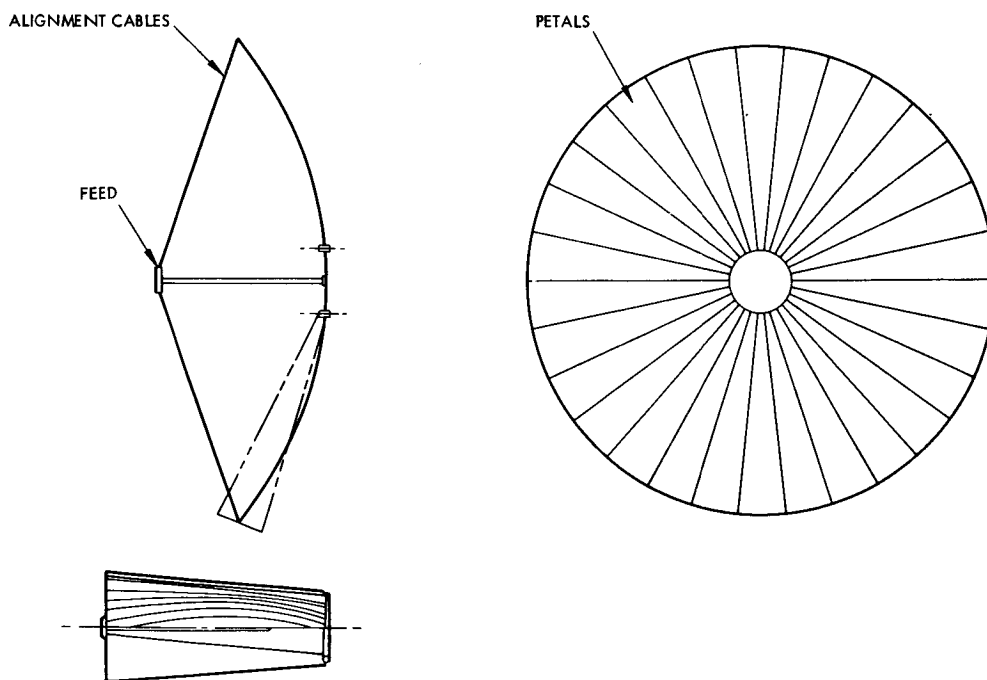


Figure D. Petaline Antenna Design Concept

ANTENNAS FOR SPACE COMMUNICATION – WEIGHT BURDENS FOR PARABOLOIDS

Antenna weight burdens are derived for extensible antennas and small (less than 10 feet equivalent diameter) antennas used as antennas on spacecraft.

The umbrella antenna design utilizes a lightweight mesh reflector spread over a framework of radial ribs. A metalized fabric or wire mesh forms a useful reflector for rf energy for an umbrella type of antenna if the mesh size is a small fraction of a wavelength. Mesh weight is minimized by selecting relatively small mesh size. This is limited by strength required for handling and deployment. Typical meshes of metalized nylon are available with a specific weight of 0.4 oz/yd². The number of ribs in an umbrella antenna influences the degree of conformity of the design to the desired paraboloidal shape.

An inflatable antenna design concept is presented for comparison which consists of a mylar aluminum sandwich material reflector similar to the material used in the ECHO II satellite. This material exhibits a degree of rigidity when stretched beyond its yield point. In order to restrain these loads in a lens shaped design, a torus support structure is required. A pressure stabilized toroidal support member is required for the initial inflation. Rigidizable materials could be used to retain strength following loss of the inflatent.¹

Petaline antenna design is the approach required for high precision and high gain applications. This is at the expense of much higher weights than are required for the umbrella or inflatable design approach. Honeycomb sandwich construction with aluminum or beryllium face sheets are one candidate construction method. Electro-deposited nickel structures are also adaptable to construction of antenna petals.

Weight estimates for antennas of different size is shown in the Figure for the three types of constructions. A 500 pound weight limit for the antenna results in a 46 foot diameter petaline antenna, a 68 foot diameter inflatable antenna, and a 120 foot diameter umbrella antenna.

In terms of the weight burdens of the overall communications system methodology the figure may be reinterpreted as given in Table I.

Since

$$W_{d_T} = K_{d_T} (d_T)^{n_T} + W_{KT}$$

where

W_{d_T} = Antenna weight (measured in pounds)

d_T = Aperture diameter (measured in cm)

¹Keller, L. B. and Schwartz, S., "Rigidization Techniques for Integrally Woven Composite Constructions," Air Force Material Laboratory Report, ML-TDR-64-299, September 1964.

K_{dT} = Constant rotating antenna weight to apertures diameter

W_{KT} = Antenna weight independent of aperture diameter (measured in pounds)

n_T = A constant

and K_{dT} , W_{KT} , and n_T are the weight burdens given by the values of Table I for large antennas, 10 to 100 feet in diameter.

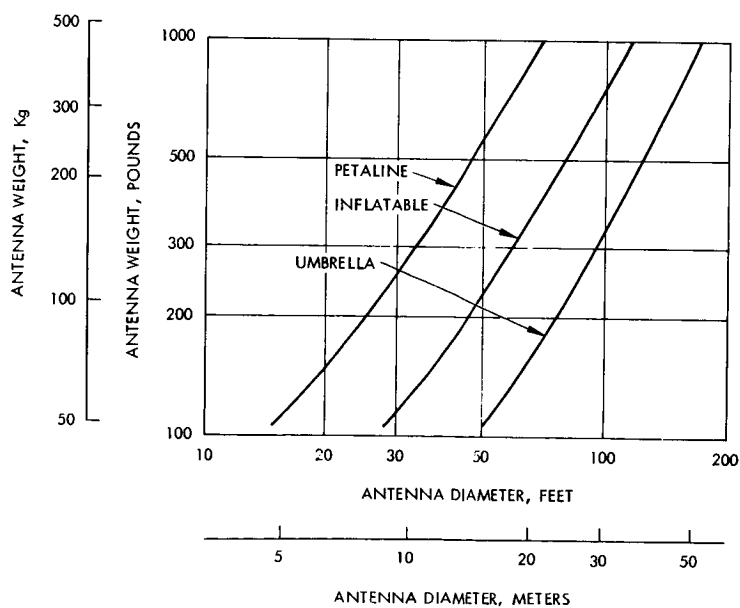
Table I. Weight Burdens

Antenna Type	K_{dT}	W_{KT}	n_T
Umbrella	0.012	42	2.2
Inflatable	0.03	105	2.2
Petaline	0.075	263	2.2

For smaller antennas, 0.5 to 10 feet in diameter, the values of Table II apply.

Table II. Weight Burdens for Small Antennas

	K_{dT}	W_{KT}	n_T
Non-extensible antennas	4.32×10^{-4}	0	2.0



Weight Comparison for Candidate Spacecraft Antenna Designs

SPECIAL PURPOSE MULTIBEAM AND SELF STEERING ANTENNAS

Several multibeam and self steering spacecraft antennas have been developed as breadboard hardware. These antennas hold special potential for near earth relay satellites rather than for high efficiency deep space antennas.

The multibeam and self steering antennas discussed briefly in this section achieve antenna gain in the desired direction with electronic means as opposed to mechanical means. These antennas fall into two generic groups: those that require external controls to properly phase the elements and those that are self steering. The externally controlled systems, such as the conventional phased array, need (1) an external sensor (i-f, r-f, or ground station), (2) a computer, (3) a phasing network, and (4) an attitude sensing device to point the beam appropriately. In the self-steering system, however, attitude information is determined by the antenna system using a pilot beam from a ground station, and internal electronic circuitry which senses the phase of incoming pilot signals to position a beam in that direction.

Three general groups of self-steerable antennas are considered potentially capable of fulfilling the characteristics dictated by the space mission. These are briefly reviewed in the following paragraphs.

Switched Multiple-Beam Antennas. This group uses multiple-beam antennas with appropriate switching and control circuitry to select the proper beam with on command from the transmitter station or as indicated by a pilot signal from the receiver station. Several configurations are possible, including multiple feed lenses, reflectors, and beam-forming matrices.

The Transdirective Array, a special configuration of the multiple-beam array. This array utilizes a hybrid beam-forming matrix and array elements to form a high-gain antenna that receives incident signals from arbitrary directions, processes them to have arbitrary amplification and frequency before reradiating the signals from the same (or another) matrix toward arbitrary, desired directions. The system selects for reception, signals from stations which identify themselves with unique pilot tones and reradiates these signals toward other stations. The re-directing of the transmitter beam is accomplished either through the use of pilot tones transmitted from the desired station or by a command signal. The participating stations all utilize the high gain and directivity of the Transdirective Array as they simultaneously communicate with one another through the spacecraft.

Self-Phasing Arrays. This group of antennas can be composed of conformal arrays of elements. Each element has its own electronic circuitry that automatically phases the elements to produce a beam in the direction dictated by a pilot signal. (The pilot signal is sent from a station desiring to communicate with a transmitting station.)

In the simplest form of the self-phasing (retrodirective array) phase inversion is needed. This is derived from a mixing action. A c-w signal received by the nth element of an array is subtracted from (mixed with) a common local oscillator to obtain a transmit signal close to the received signal except that it has an inverted phase angle. The phase angle is similarly inverted at every element to create the condition by which

the transmit signal is formed into a beam essentially in the same direction as the received signal. A circulator or branching filter is used to separate the transmit and receive signals at the antenna elements. A slight frequency shift is used to improve isolation between transmitted and received signals and to make provision for suitable amplification.

In a more advanced form of this idea, the total incoming signal at the n th element consists of a narrow band pilot signal (ω_{p1}), offset from a broad information band (ω_m). The signals are subtracted from a suitable offset frequency (ω_1) and the difference frequencies are filtered, separately amplified, and mixed once more. The signal at the difference frequency ($\omega_m - \omega_{p1}$) is independent of the incoming interelement phase shift and is summed with all similar outputs from the other elements. At this point, the total array gain is realized.

A pilot (ω_{p2}) transmitted from the receiving ground station is also processed to form a beam toward that station. The information from the ground transmitting station, which was summed and amplified is now frequency translated and added to the pilot signal (ω_{p2}) to send the information toward the receiving station. Thus a complete communication channel is established electronically.

Adaptive Arrays. This class of arrays is closely related to self phasing arrays but uses phase-locked loops at each element to accomplish the appropriate phasing across the antenna aperture. The term "adaptive" comes from the adaptive properties of the phase locked loops which adjust the phase out of each element to a standard reference. This allows the signals to be added in phase and to realize the maximum gain of the array regardless of the direction of the incoming signal. Adaptive arrays can be made to transmit retrodirectively by appropriate additions to the circuitry at each element.

HIGH GAIN, SELF-STEERING ANTENNA SYSTEM FOR SATELLITE-EARTH COMMUNICATIONS

A description of a self-steering spacecraft antenna system is given. Antenna gain of 29.8 db may be pointed electronically at any point within a 30 degree cone.

An engineering model of a self-phasing antenna system for satellite-earth communications has been designed and fabricated at the Hughes Aircraft Company (NAS 5-10101). This system, shown in block diagram in Figure A, incorporates two channels, each with a 125-MHz RF bandwidth (for the sake of clarity, only one channel is illustrated completely in the figure). The system is designed to receive at 8 GHz and transmit at 7.3 GHz. The design is based on application to a gravity-gradient oriented and stabilized satellite in synchronous orbit with a conical coverage angle of ± 15 degrees. This coverage allows for uncertainties in the attitude of the spacecraft. The transmitting and receiving portions will steer appropriate beams along arbitrary directions within that cone. Two independent channels will be included which provides four independent steered beams. The beam designations and the frequency bands utilized are shown in Figure B.

This system is intended to serve as a communication link to relay information transmitted from one station to another station via high-gain beams. The positions of these beams are controlled by the phase information obtained from CW pilot signals which are generated by the ground stations which communicate to one another through the relay satellite.

For the channel shown in Figure A, a receiving pilot, a transmitting pilot, and a modulated signal are received by the receiving element, passed through a high-pass filter, down-converted to an intermediate frequency, and amplified by a wide-band IF preamplifier. After pre-amplification, the information signal and the pilots are separated by means of a triplexer filter. The pilots are then down-converted to a second, lower, IF to allow utilization of very narrow-band-pass filters to establish a good signal-to-noise ratio for the pilots. These band-pass filters comprise the quadruplexer which, in addition to limiting the noise bandwidth of the pilot channels, serve to separate the pilot signals. After passing through the quadruplexer, the pilot signals are up-converted to about 200 MHz to enable these pilots to be mixed with the wide-band modulated signals without overlap of the power spectra.

With reference to Figure A, the modulated signal, 450 to 575 MHz, passes from the triplexer to a wide-band mixer, and the receiving pilot signal, 206 MHz, also passes to this mixer. The modulated signal is denoted by $\cos \{[\omega_c + f(t)]t - \phi_i\}$ and the pilot signal by $\cos [\omega_p t - \phi_i + \beta]$, where ω_c is the carrier frequency, ω_p is the pilot frequency, $f(t)$ is a modulating signal, ϕ_i is the phase angle of the received signal relative to an arbitrary reference for the i^{th} element, and β is the phase shift of the pilot signal relative to the modulated signal, common for all elements. If these two signals are mixed and the lower sideband retained, there results $\cos \{[\omega_c - \omega_p + f(t)]t - \beta\}$; therefore, it is seen that the phase of the resultant IF signal is independent of the relative phase angle of the signals at the elements. The signals from the output of these mixers, (one for each element) which are in phase, are summed. At the point of summation, the receiver array gain is realized for the information signals.

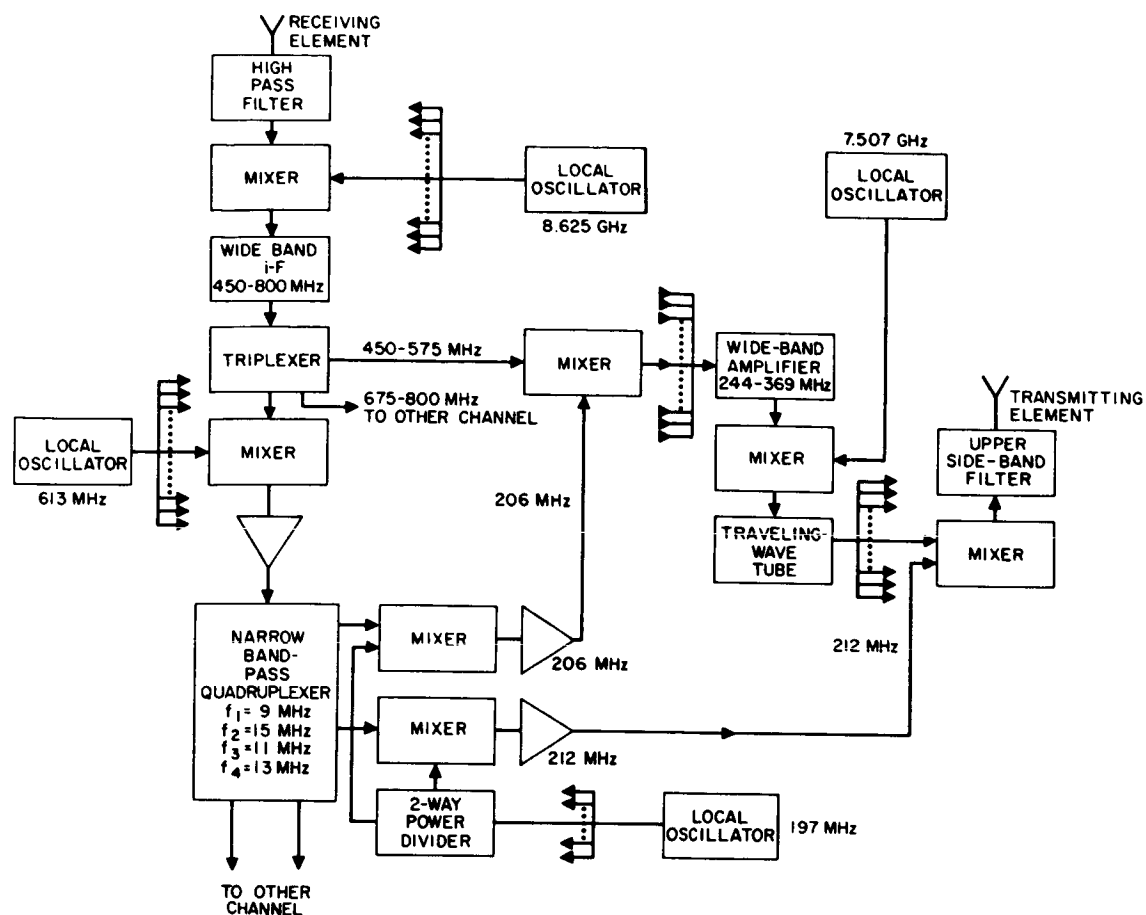


Figure A. High-Gain , Self-Steering Engineering Model Schematic

HIGH GAIN, SELF-STEERING ANTENNA SYSTEM FOR SATELLITE-EARTH COMMUNICATIONS

The signal is then amplified at IF, up-converted to RF, amplified at RF, and then distributed to the final transmitting mixers. At these mixers the transmitting pilot is mixed with the modulated signal and the upper sideband is selected by the band-pass filter that follows. A modulated signal is produced at a transmitting element; this signal has a phase angle which has the opposite sense from the phase angle of the transmitting pilot at the corresponding receiving element. The condition necessary to transmit the information from the antenna system in the direction of the transmitting pilot is that the recovery and transmitting arrays be scaled in wavelength.

The Table presents the electrical and physical characteristics of the engineering model, and the projected characteristics for a flight model of a similar system. Figure C shows the configuration for an engineering model. The flight model will be configured similarly.

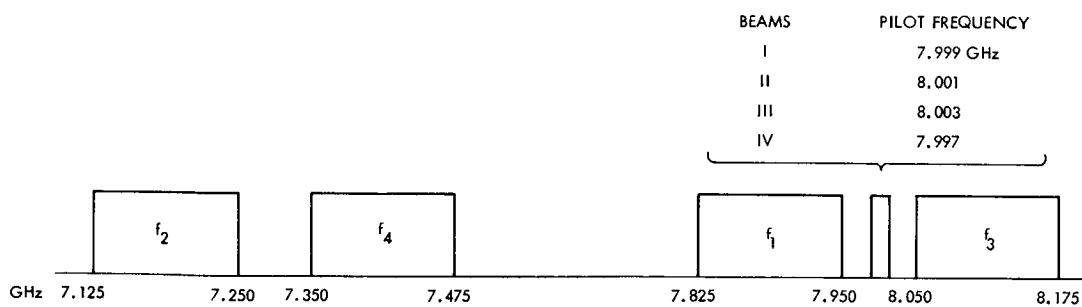
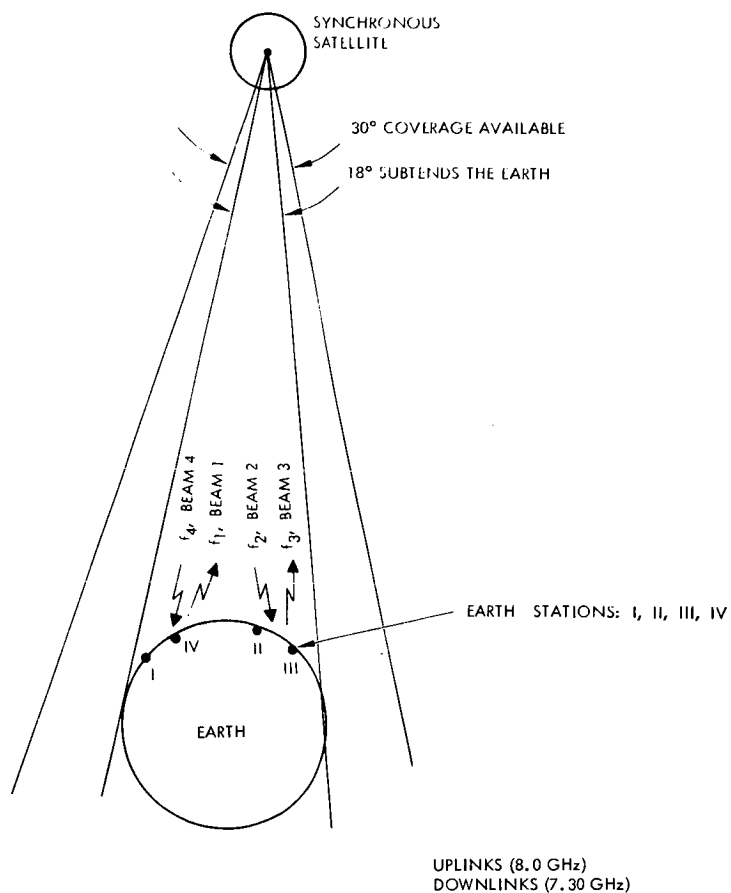


Figure B. Synchronous Altitude Gravity-Gradient 30-Degree Cone of Coverage

Transmitting and Receiving Apertures
Radio Frequency Antennas

HIGH GAIN, SELF-STEERING ANTENNA SYSTEM FOR SATELLITE-EARTH
COMMUNICATIONS

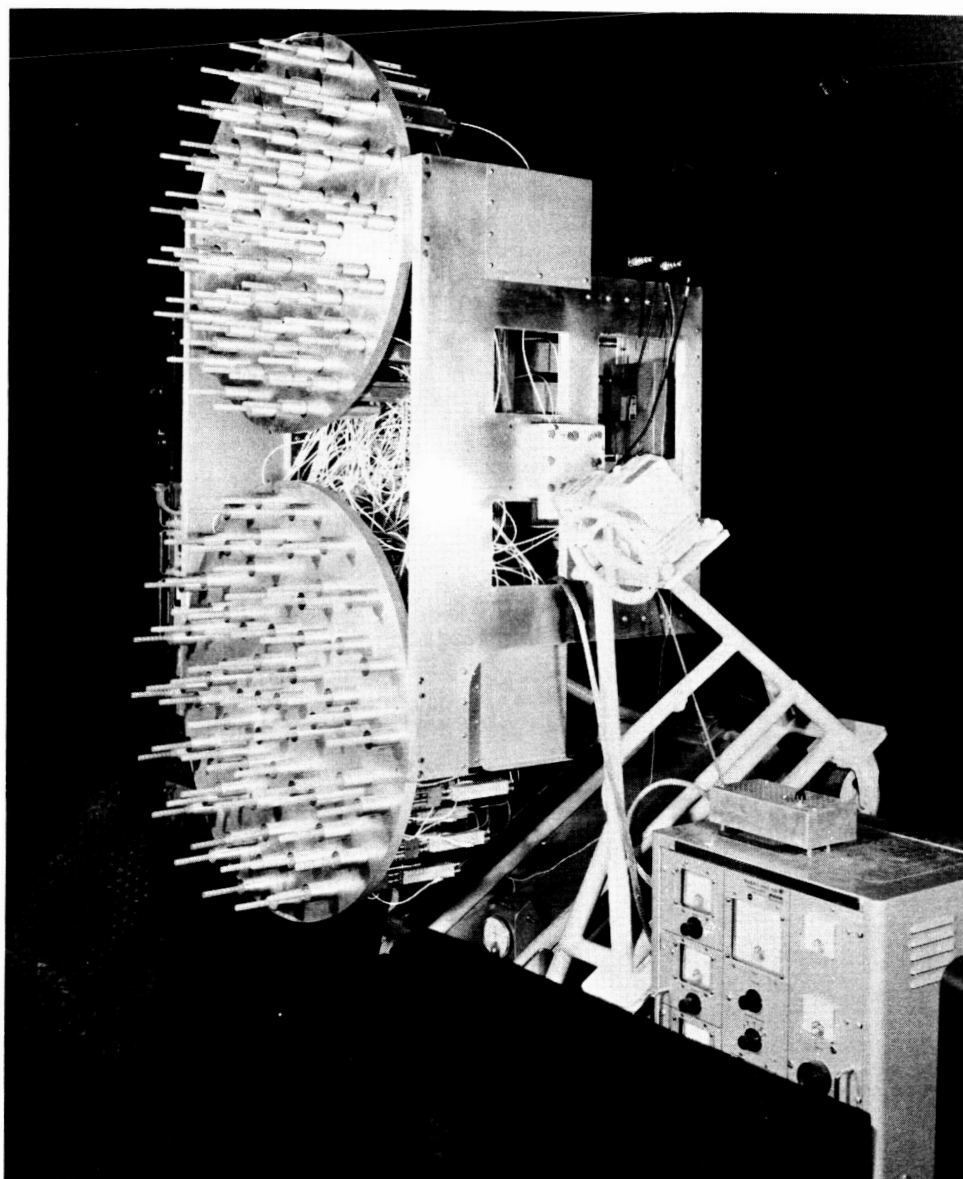


Figure C. Engineering Model of Self Steering Antenna

Characteristics of the Repeater

Parameter	Design Goals for Engineering Model	Measured Performance	Projected Characteristics of Flight Model
Number of elements, each for two arrays	64		64
Number of channels	2		2
R-f bandwidth, each channel	125 MHz		125 MHz
Guard band, between channels	100 MHz		100 MHz
Total cone angle of coverage	30 degrees	30 degrees	30 degrees
Element gain, minimum	11.6 db	12.4 db	11.6 db
Array gain, minimum	29.8 db	30.4 db	29.8 db
Polarization	Circular	Circular axial ratio = 0.8 db	Circular
Average mixed-filter pre- amplifier noise figure	15.2 db (max)	14.4 db	7 db
Effective radiated power	28.0 dbw	27.8 dbw	35.0 dbw
Ratio of pilot to modulated signal power when 125 MHz bandwidth is utilized	-10 db	*	-10 db
Power consumption: receiver	32.0 watts excluding L. O.		21.5 watts including L. O.
Power consumption: pilot processor	108.7 watts	182.6 watts	108.7 watts
Power consumption: attitude readout	0.9 watt		0.9 watt
Power consumption: total transmitter	201.1 watts excluding L. O.	87.9 watts** excluding L. O.	204.5 watts including L. O.
Prime power (exclusive of power supplies)	342.7 watts	270.5 watts	335.6 watts
Power consumption power supplies	—	—	73.3 watts
Power consumption: total prime power	—	—	408.9 watts
Total weight		180.0 Kg	79.0 Kg
<p>* Pilot signal ratios much lower than the design values were measured in the T-V tests (see discussion).</p> <p>** Power consumption applies to one channel of transmitter. For the channel operation less than twice this value would be needed.</p>			

ANTENNAS FOR SPACE COMMUNICATION – SURFACE STATION COST BURDENS

Surface station cost burdens are based on the cost of the DSIF antennas.

The cost to construct a surface station antenna has been evaluated as a function of antenna diameter. The cost evaluation has been made compatible with the communications system methodology developed under this contract and used to evaluate different communications systems.

The relationship used by the communication system methodology to relate surface station antenna cost to antenna diameter is as follows:

$$C_{\theta_R} = K_{\theta_R} (d_R)^{m_R} + C_{KR}$$

where

C_{θ_R} = the antenna fabrication cost

K_{θ_R} = a constant relating antenna diameter to cost

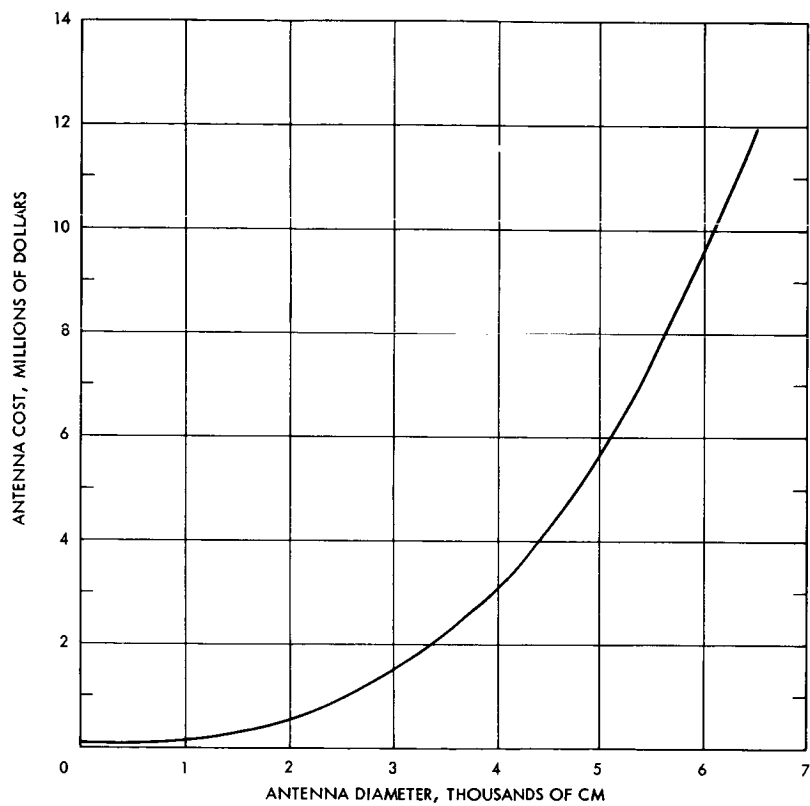
d_R = the receiver antenna diameter

m_R = a constant

C_{KR} = a fixed cost independent of antenna

The burden relationships are a function of frequency. Since 2.3 GHz is the assigned deep space communication frequency, the burdens, K_{θ_R} , m_R , and C_{KR} have been evaluated at this frequency. The data used in this evaluation is the cost data of the DSIF 85 foot and 210 foot antennas. The cost for these antennas are \$980,000 and \$12,000,000 respectively. These values are related by the diameter to the 2.8 power. These will be a certain amount of fixed cost for each station site (represented by C_{KR}), this is taken to be \$100,000 for a generalized surface station. Combining this value with the DSIF data gives values for the surface receiving aperture as indicated in the table. This relationship is plotted in the Figure.

Burden Constant	Surface Station Antenna Burdens	
	Antenna Diameter in cm	Antenna Diameter in feet
C_{KR}	100,000	100,000
m_R	2.8	2.8
K_{θ_R}	2.5×10^{-4}	3.5



Earth Station Antenna Costs

ANTENNAS FOR SPACE COMMUNICATION – SPACECRAFT COST BURDENS

Cost burdens for spacecraft antennas are documented which are suitable for use in the Communication System Methodology developed for this contract.

The cost to fabricate an antenna for spacecraft has been evaluated as a function of the antenna diameter. These relationships, with many similar ones for other parts of a deep space communications link, are used to determine the optimum values of spacecraft and surface station antenna size to provide a minimum cost system.

The relationship used in the antenna cost modeling is:

$$C_{\theta T} = K_{\theta T} (d_T)^{m_T} + C_{KT} \quad (1)$$

where

$C_{\theta T}$ = the transmitting antenna cost

$K_{\theta T}$ = a constant relating transmitting antenna fabrication cost to diameter

d_T = the transmitting antenna diameter

m_T = a constant

C_{KT} = the transmitting antenna fabrication cost independent of aperture diameter.

It is required then to provide values for the three burden constants used in equations 1: $K_{\theta T}$, m_T , and C_{KT} .

These constants are derived from two basic sources. The first source is the cost data that may be obtained from the construction of mechanical structures similar to antennas and the second source is the actual construction costs for spaceborne antennas.

The antenna costs used for the communications system methodology are the costs for a single antenna with engineering development costs prorated over several antennas. Table I contains representative cost data for large spaceborne antennas, including the development costs. The costs may be interpreted in terms of the burdens for spacecraft transmitting antennas as indicated in Table II for 10 antennas and 15 antennas. These costs are for large extensible antennas. Burden costs for small (less than 10 feet equivalent diameter) spaceborne antennas are given by the burden values of Table III for planar arrays and parabolic dishes, the Figure has plots of the values of cost for these several antennas.

Table I. Cost Size Relationships for Large Spaceborne Antennas

Item	Remarks	Cost Dollars	
		Diameter d, in Feet	Diameter, d, in cm
Engineering	Fixed Cost 20 man years	600,000	600,000
Tooling	Surface dependent	$500d^2$	$0.538d^2$
Fabrication	Surface dependent	$170d^2$	$0.183d^2$
Material	Surface dependent	$10d^2$	$0.0106d^2$
Quality Control	Surface dependent	$80d^2$	$0.086d^2$
Handling and	Volume dependent	$0.5d^3$	$1.76 \times 10^{-5}d^3$

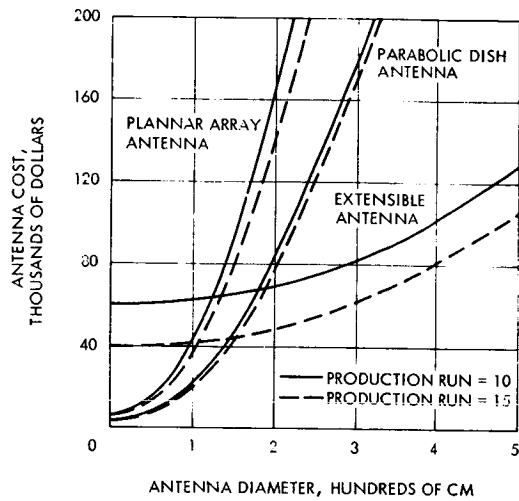
Table II. Antenna Burdens for Large Extensible
Spacecraft Antennas

Burden Constant	10 Antennas Constructed		15 Antennas Constructed	
	Diameter in cm	Diameter in Feet	Diameter in cm	Diameter in Feet
K_{θ_T}	0.084	150	0.08	143
C_{K_T}	60,000	60,000	40,000	40,000
m_T	2.19	2.19	2.19	2.19

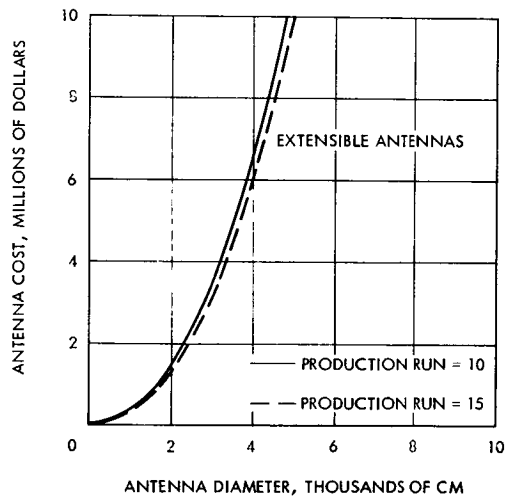
ANTENNAS FOR SPACE COMMUNICATION – SPACECRAFT COST BURDENS

Table III. Antenna Burdens for Small Spacecraft Antennas

Burden Constant	10 Antennas Constructed		15 Antennas Constructed	
	Diameter in cm	Diameter in Feet	Diameter in cm	Diameter in Feet
(a) Planar Array				
K_{θ_T}	4	3710	3.4	3160
C_{KT}	5000	5000	5000	5000
m_T	2	2	2	2
(b) Parabolic Dish				
K_{θ_T}	2	1850	1.92	1780
C_{KT}	2500	2500	2500	2500
m_T	2	2	2	2



(a)



(b)

Cost of Spacecraft Transmitting Antennas

TRANSMITTING AND RECEIVING APERTURES

Optical Frequency Apertures

	Page
Introduction	282
Optical Configurations	284
Optical Configurations — Optics with a Large Field of View	286
Optical Configurations — Use of a Tracking Mirror	290
Optical Configurations — Reflectance and Attenuation in Optical Systems	292

INTRODUCTION

Subsequent subtopics include: optical configurations, manufacturing techniques and tolerances, and material choices for optical beamwidths from 1 to 100 microradians.

The optics used in a laser communications system are a major design consideration. To obtain improved communication system performance using optical wavelengths requires each area of the technology to be examined such that potential implementation choices, basic limitations and interface requirements be understood.

The material of this section is organized in the following manner: The first subsection deals with optical configurations and the concomitant tolerances of such configurations. The next subsection deals with manufacturing techniques and thermal considerations while the third subsection deals with implementation factors such as material choices and their associated weight and cost.

The optical transmission aperture must provide a beam which is as narrow as possible to concentrate the transmitted energy at the receiver. This beamwidth produces one of the most difficult problems for optical communications and is therefore examined briefly below.

The beam spread of a perfect, unobstructed optical system can be depicted by a plot of the Airy Disk shape where the abscissa would be intensity of the energy and the ordinate would be the angular spread. The angular spread as measured by the diameter of the first ring of zero energy would be given by

$$\theta = \frac{2.44\lambda}{D} \quad (1)$$

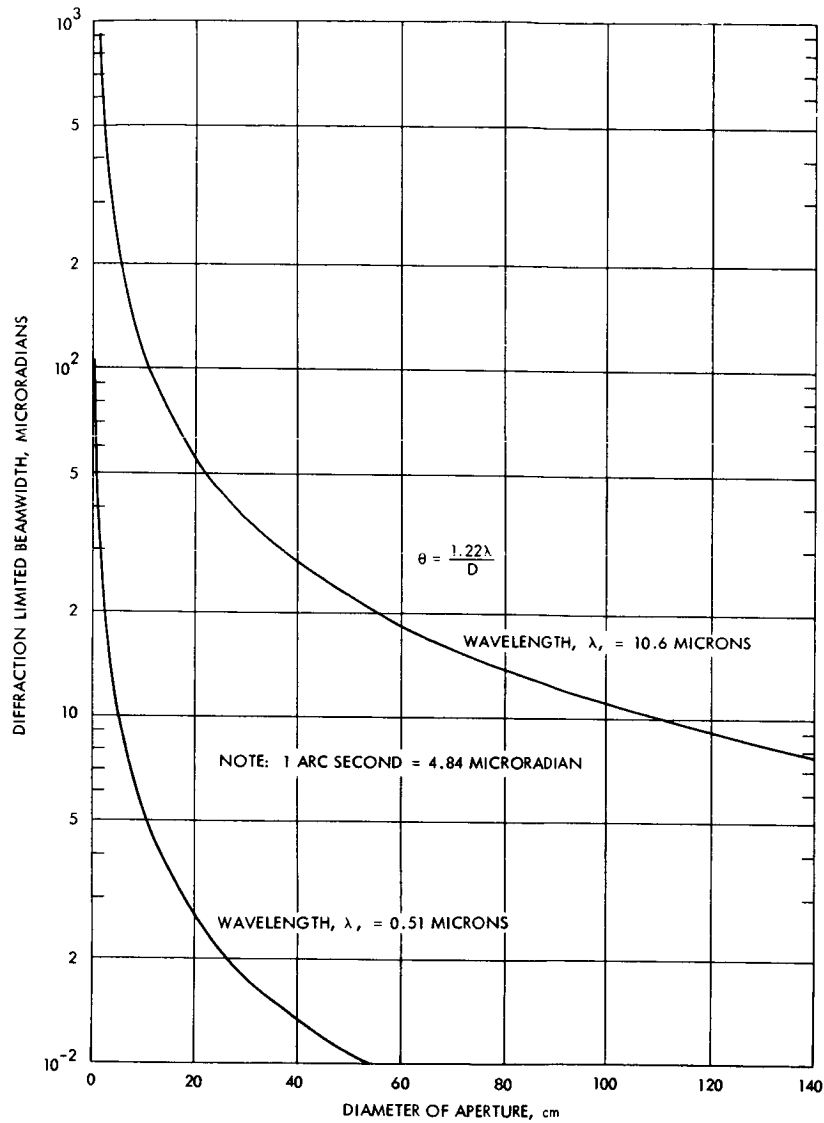
where

θ is the angular spread, radians

λ is the wave length

D is the aperture diameter

In practice however, the angular diameter that is useable is necessarily less than this and is taken at the half power points to be $\theta = 1.04\lambda/D$. (Another measure sometimes used for measuring beamwidths is the resolution of the aperture. Two adjacent point sources are considered to be resolvable when separated by $\theta = 1.22\lambda/D$.) The fact that the beam spread is inversely proportional to the aperture favors the use of a large diameter transmission unit. The narrow beamwidths of diffraction limited optics place severe pointing problems on the pointing and tracking system. As a measure of the pointing accuracy required, the diffraction limited beamwidth is plotted in the figure as a function of aperture for 0.51 and 10.6 microns. These results are possible only for excellent seeing when using the larger diameters. Such seeing may well be found only outside the Earth's atmosphere. As is seen from the figure, beamwidths as small as 1 microradian may be considered for visible light, beamwidths in the order of tens of microns are more appropriate for 10.6 micron transmission.



Diffraction Limited Beamwidths at
Optical Frequencies

Transmitting and Receiving Apertures Optical Frequency Apertures

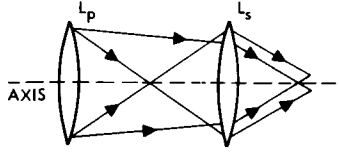
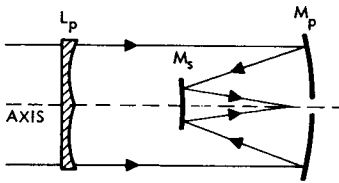
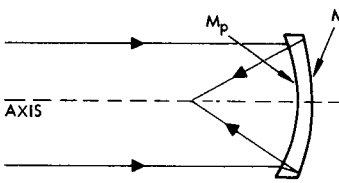
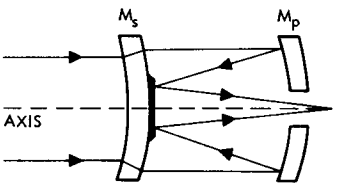
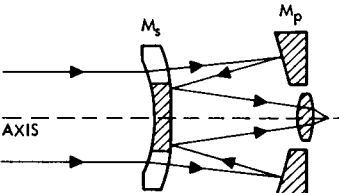
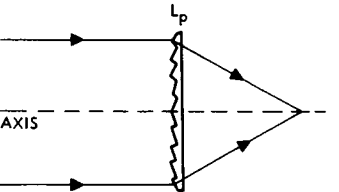
OPTICAL CONFIGURATIONS

Thirteen optical systems are shown in tabular form and pertinent design characteristics are given.

Optical Systems

TYPE	RAY DIAGRAM	OPTICAL ELEMENTS	PERTINENT DESIGN CHARACTERISTICS
PARABOLOID		REFLECTIVE M_p = PARABOLOIDAL MIRROR	<ol style="list-style-type: none"> 1. FREE FROM SPHERICAL ABERRATION. 2. SUFFERS FROM OFF-AXIS COMA. 3. AVAILABLE IN SMALL AND LARGE DIAMETERS AND f/NUMBERS. 4. LOW IR LOSS (REFLECTIVE). 5. DETECTOR MUST BE LOCATED IN FRONT OF OPTICS.
CASSEGRAIN		REFLECTIVE M_p = PARABOLOIDAL MIRROR M_s = HYPERBOLOIDAL MIRROR	<ol style="list-style-type: none"> 1. FREE FROM SPHERICAL ABERRATION. 2. SHORTER THAN GREGORIAN. 3. PERMITS LOCATION OF DETECTOR BEHIND OPTICAL SYSTEM. 4. QUITE EXTENSIVELY USED.
GREGORIAN		REFLECTIVE M_p = PARABOLOIDAL MIRROR M_s = ELLIPSOIDAL MIRROR	<ol style="list-style-type: none"> 1. FREE FROM SPHERICAL ABERRATION. 2. LONGER THAN CASSEGRAIN. 3. PERMITS LOCATION OF DETECTOR BEHIND OPTICAL SYSTEM. 4. GREGORIAN LESS COMMON THAN CASSEGRAIN.
NEWTONIAN		REFLECTIVE M_p = PARABOLOIDAL MIRROR M_s = REFLECTING PRISM OR PLANE MIRROR	<ol style="list-style-type: none"> 1. SUFFERS FROM OFF-AXIS COMA. 2. CENTRAL OBSTRUCTION BY PRISM OR MIRROR.
HERSCHELIAN		REFLECTIVE M_p = PARABOLOIDAL MIRROR INCLINED AXIS	<ol style="list-style-type: none"> 1. NOT WIDELY USED NOW. 2. NO CENTRAL OBSTRUCTION BY AUXILIARY LENS. 3. SIMPLE CONSTRUCTION. 4. SUFFERS FROM SOME COMA.
SCHMIDT		REFLECTIVE-REFRACTIVE M_p = SPHERICAL MIRROR M_s = REFRACTIVE CORRECTOR PLATE	<ol style="list-style-type: none"> 1. PRODUCES A CURVED FIELD. 2. FREE OF SPHERICAL ABERRATION AND COMA. 3. CENTRAL OBSTRUCTION BY ITS OWN FIELD SURFACE. 4. CAN OBTAIN LOW f/NUMBER. 5. SHARPER FOCUS OVER LARGER AREA THAN PARABOLOID. 6. MAY BE BUILT AS SOLID UNIT.
GALILEAN		REFRACTIVE L_p = BICONVEX LENS L_s = BICONCAVE LENS	<ol style="list-style-type: none"> 1. RADIATION GATHERING POWER LESS THAN REFLECTION SYSTEMS. 2. RELATIVELY SHORT LENGTH. 3. LIMITED FIELD OF VIEW. 4. SPECTRAL RESPONSE LIMITED BY LENS MATERIAL.

Optical Systems (continued)

KEPLERIAN		REFRACTIVE L_s = BICONVEX LENS L_p = BICONVEX LENS	<ol style="list-style-type: none"> 1. RADIATION GATHERING POWER LESS THAN REFLECTION SYSTEMS. 2. SPECTRAL RESPONSE LIMITED BY LENS MATERIAL. 3. NOT WIDELY USED NOW.
SCHMIDT-CASSEGRAIN OR BAKER		REFLECTIVE-REFRACTIVE M_p = ASPHERIC MIRROR M_s = ASPHERIC MIRROR L_p = REFRACTIVE CORRECTOR PLATE	<ol style="list-style-type: none"> 1. PRODUCES FLAT FIELD. 2. VERY SHORT IN LENGTH. 3. COVERS LARGE FIELD. 4. CORRECTOR PLATE HAS LARGER CURVATURE THAN SCHMIDT.
MANGIN MIRROR		REFRACTIVE-REFLECTIVE M_p = SPHERICAL REFRACTOR M_s = SPHERICAL REFLECTOR	<ol style="list-style-type: none"> 1. SUITABLE FOR IR SOURCE SYSTEMS. 2. FREE OF SPHERICAL ABERRATION AND COMA 3. MOST SUITABLE FOR SMALL APERTURES. 4. COVERS SMALL ANGULAR FIELD. 5. USES SPHERICAL SURFACES.
MAKSUTOV		REFRACTIVE-REFLECTIVE M_p = MENISCUS REFLECTOR M_s = MENISCUS REFRACTOR-REFLECTOR	<ol style="list-style-type: none"> 1. FREE OF SPHERICAL ABERRATION, COMA, AND CHROMATISM. 2. VERY COMPACT. 3. LARGE RELATIVE APERTURE. 4. MAY ALSO USE COMBINATIONS OF SPHERICAL AND ASPHERIC ELEMENTS.
GABOR		REFRACTIVE-REFLECTIVE M_p = SPHERICAL REFLECTOR M_s = SPHERICAL REFRACTOR-PLANO REFLECTOR	<ol style="list-style-type: none"> 1. HIGH APERTURE SYSTEM. 2. HAS MEAN CORRECTION OF SPHERICAL ABERRATION AND COMA. 3. SUITABLE FOR IR SOURCE SYSTEMS.
FRESNEL LENS		REFRACTIVE L_p = SPECIAL FRESNEL LENS	<ol style="list-style-type: none"> 1. FREE OF SPHERICAL ABERRATION. 2. INHERENTLY LIGHTER WEIGHT. 3. SMALL AXIAL SPACE. 4. SMALL THICKNESS REDUCES INFRARED ABSORPTION. 5. DIFFICULT TO PRODUCE WITH PRESENT INFRARED TRANSMITTING MATERIALS.

OPTICAL CONFIGURATIONS – OPTICS WITH A LARGE FIELD OF VIEW

Optical systems having a field of view larger than beamwidth are examined for suitability to laser communications.

The previous topic noted the narrow beamwidths (and consequent accurate pointing requirements) of optical frequency apertures. This topic gives optical configuration choices which may be considered in meeting the requirements of optical frequency communication.

Because of the need to track with extremely small angular errors, it is quite desirable to design a system in which the fine pointing is accomplished by movement of small elements of the system, rather than movement of the entire system. This can be accomplished in one of three ways.

1. A larger field of view than is necessary can be provided and the transmitter source and receiver detector can be moved in the focal plane for tracking.
2. A reimaging optical system can be made with a small transfer lens that moves to provide fine pointing.
3. The optical system can incorporate a space of collimated light in which a mirror is inserted. Control of the mirror motion would control the image position in receiving, or the beam direction of a transmitter.

The first of these pointing methods is discussed below. The second is discussed extensively in the next Part of this Volume, Acquisition and Tracking. The third way is discussed in the next topic.

If the receiver and transmitting units are moved in the focal plane, there is a relatively wide choice of available systems. It is desirable, for thermal reasons, to keep the focal plane location away from the critical structure controlling alignment. This factor would perhaps favor a Cassegrain configuration, over a Newtonian configuration. In addition, the Cassegrain's shorter structure, lighter weight and lower moment of inertia favor the use of a Cassegrain over a Gregorian. The diameter of the diffraction limited field of Newtonian telescope – defined as that field where the length of the coma (see definition of coma below) is less than the Airy disc diameter – is about the same as a Cassegrain of equivalent focal ratios and is given by:

$$h = 30 \lambda f^3 \quad (10-2)$$

where:

h is field diameter

λ is wave length

f is focal ratio

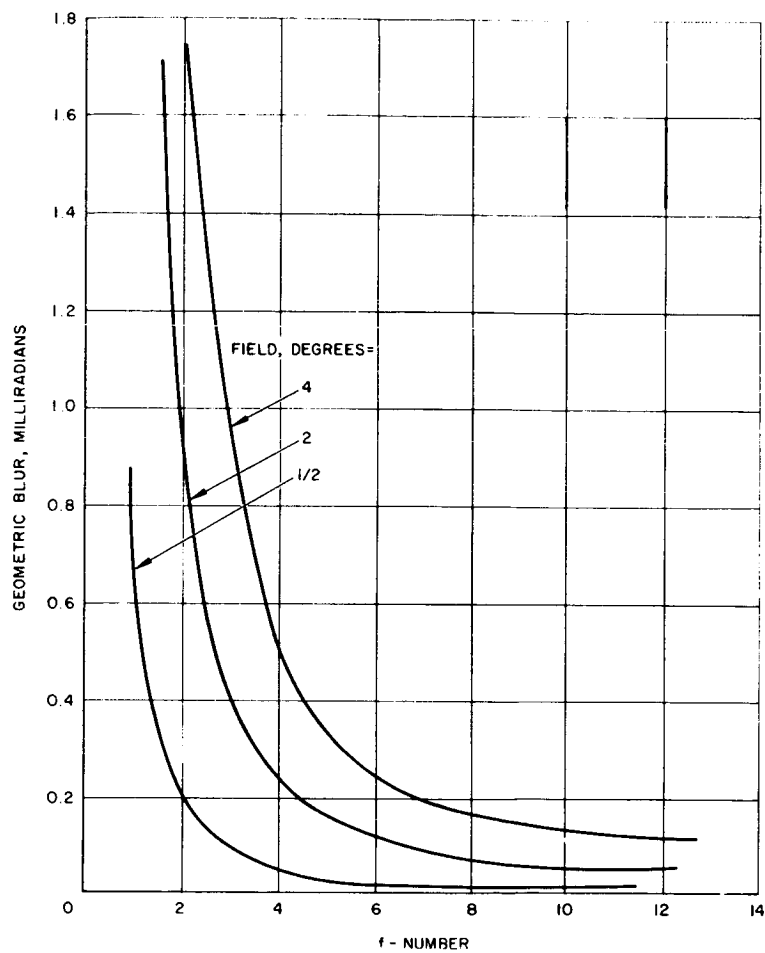


Figure A. Coma and Astigmatism Aberrations of a Parabolic Reflector Off Axis, Versus f Number

OPTICAL CONFIGURATIONS – OPTICS WITH A LARGE FIELD OF VIEW

Geometric blur is one of the penalties for off axis tracking. Figure A plots geometric blur due to coma and astigmatism versus f-number as a function of field of view for 0.51 microns. These plots strictly hold for only parabolic systems. Figure B compares the geometric blur circle of several types of telescopic systems at varying angular distances off-axis. Chosen for each category are typical examples found in use today. The f-number of these examples vary so that the comparison is not a strict one.

Parabolic types are represented by an f-10 instrument after K. Schwarzschild in "Telescopes & Accessories" by Baker.

The Ritchey-Chretien system is an f/15 telescope discussed in "Sky & Telescope" for April 1962. The Dall Kirkham system is also an f/15 telescope discussed in the same reference.

The parabolic telescope with a Ross Corrector is the 200" Hale telescope operating at about f/4, discussed in "Telescopes" by Kuiper.

The three catadioptric telescopes (the classical Schmidt, the Maksutov-Bouwers, and the compound catadioptric) are all f/2 systems discussed by Bouwers in "Achievements in Optics". The compound catadioptric is a corrected concentric arrangement employing both a meniscus lens and a Schmidt plate.

The Ritchey-Chretien is of the Cassegrain type, but uses an approximately hyperboloidal primary mirror (with greater asphericity than the paraboloidal mirror of the Cassegrain of the same speed) to achieve a larger field. The coma of a Cassegrain system is equal to the equivalent focal length Newtonian while the astigmatism would be that of the equivalent Newtonian multiplied by the magnification of the Cassegrain secondary. These data come primarily from K. Schwarzschild as reported in "Telescopes & Accessories" by Baker. The coma alone, in radians, equals:

$$\text{Coma} = \frac{0.1875\phi}{(efl/D)^2} = \frac{0.1875\phi}{f^2} \quad (10-3)$$

where ϕ is the half field angle in radians.

efl is the effective focal length

D is the aperture diameter

f is the f-number

This is plotted in Figure C.

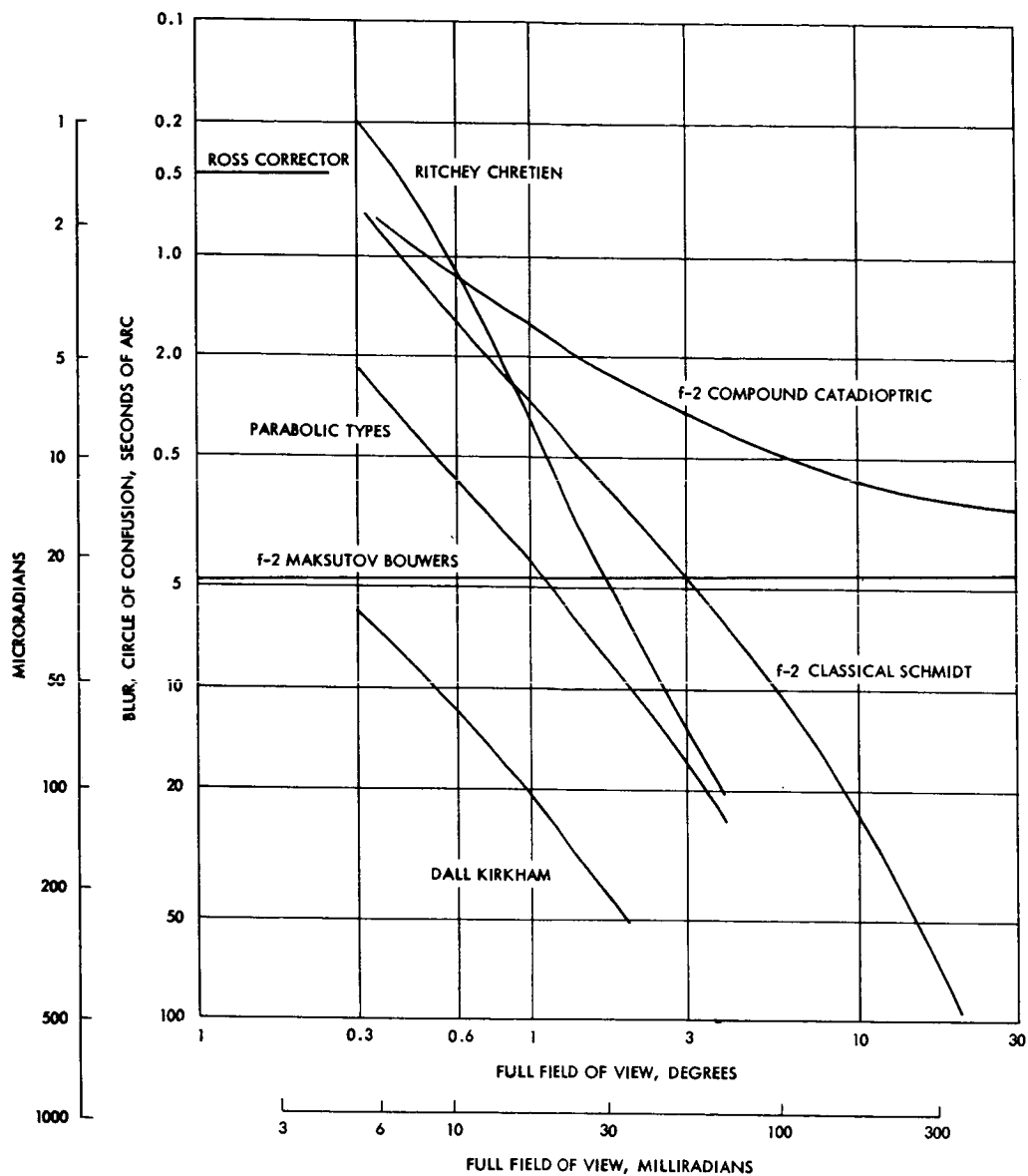


Figure B. Geometric Blur of Various Types Versus Field of View

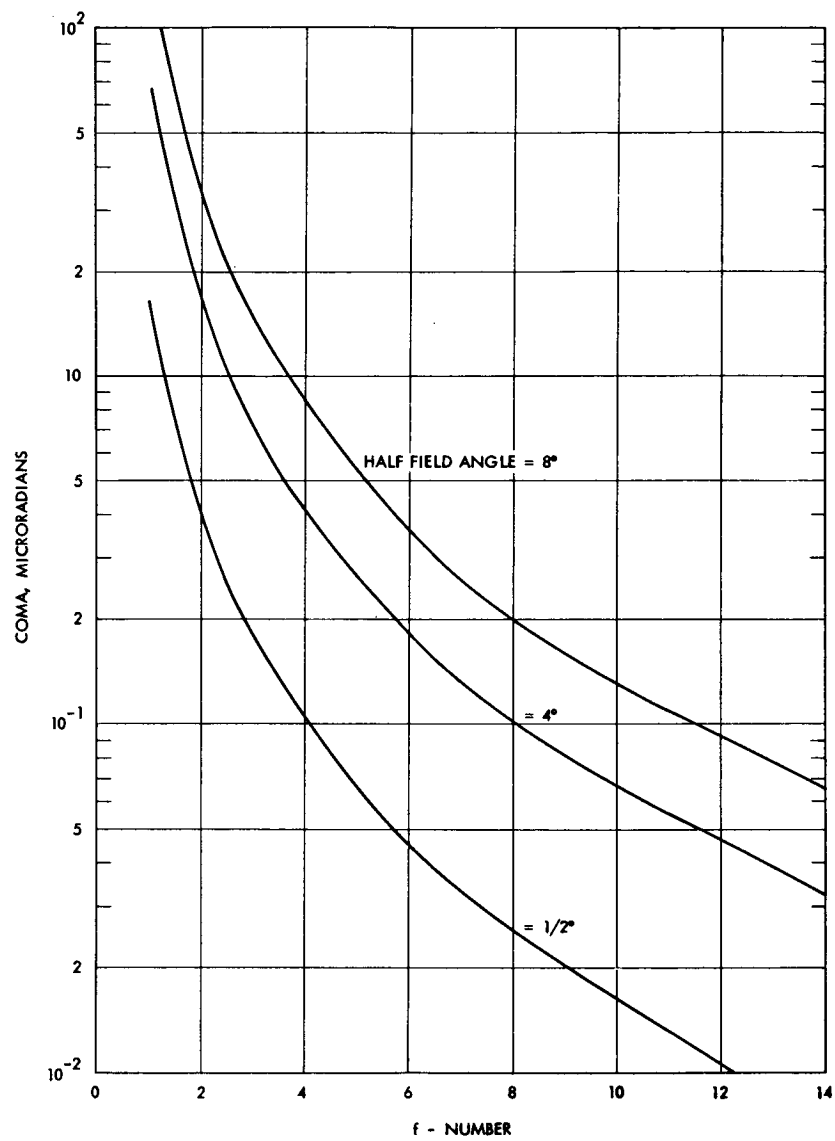


Figure C. Coma of a Cassegrain System

OPTICAL CONFIGURATIONS - USE OF A TRACKING MIRROR

Using a tracking mirror placed in collimated light a space of collimated light is very advantageous when using a mirror for fine pointing in an optical communication link.

If the spacecraft has vibration sources, tracking may be accomplished by using a space of collimated light into which a mirror is inserted. This has an added advantage in that the collimated space can also serve as a "soft link" and allow relative motion between the large optical system and the spacecraft. The situation is similar to that of a hand held telescope with an eyepiece providing collimated light. If the tracking mirror in the collimated space can remove image motion at the focal plane, large relative motions can be tolerated.

In a telescope using a mirror in a collimated space, there will be angular magnification proportional to the ratio of the aperture of the telescope to the aperture of the collimated space. Because of this, the guiding mirror must deviate the beam by an amount equal to the input error times the magnification. This reduces the sensitivity to the roughness or the error in mirror positioning and makes the sensing of the tracking signal probably the most critical item.

In summary, the three methods of providing fine guiding without pointing the entire telescope require a larger field than will actually be used. The only real field requirement of the system is that of the lead angle due to the relative velocities of the sending and receiving stations. The amplitude of the fine guidance system is bounded by the field of the telescope.

In a communication mode, an optical system would handle only monochromatic light. While there may be two different wave lengths for the transmitting and receiving functions, the optical system still need not be designed to function over a broad spectrum unless it is to serve other purposes in addition to communications. This gives the optical designer the freedom to design catadioptric systems for example without consideration of secondary color, which is the usual limiting factor in system performance.

OPTICAL CONFIGURATIONS – REFLECTANCE AND ATTENUATION IN OPTICAL SYSTEMS

Reflectance and attenuation values are given for visible and 10.6 micron radiation.

From the optical design point of view, the main effect of a change to 10.6 μ from visible optical wavelengths is that of the materials required for the refracting elements. Figure A shows the attenuation of a typical refracting or photographic type telescope due to its having glass components. A list of materials suitable for use at infrared wavelengths is given in the Table. It is immediately apparent that a system designed for 10.6 μ would be primarily a reflector.

Figure B shows the efficiency of a typical reflecting telescope due to the reflective coatings on its mirrors.

Figure C illustrates the difference in the reflectivity of both aluminum and silver coatings and their dependence on the orientation of the plane of polarization.

Optical Materials

Material	Transmission Range, Microns	Refractive Index at Midpoint of Transmission Range	Transmittance, Percent	Diameter, Inches	1 in. dia x 0.040 in. Unpol. Substrate, Typical Price, Dollars	Water Solubility gm/100 gm Water
Irtran 1	0.5-9.	1.31	90.	8.	37.00	Insoluble
Irtran 2	0.7-14.5	2.20	75.*	8.	35.00	Insoluble
Irtran 3	0.4-11.5	1.35	90.	6.	62.00	Practically insoluble
Irtran 4	0.5-22.	2.40	70.*	6.	84.50	Insoluble
Irtran 5	0.4-9.5	1.62	80.*	6.	75.50	Insoluble
Irtran 6	1.5-31.	2.71	65.*	3.	209.00	Insoluble
Calcium fluoride	0.13-12.	1.42	95.	7.	3.20	0.002
Calcium fluoride (rare earth free)	0.13-12.	1.42	95.	7.	9.00	0.002
Barium fluoride	0.15-15.	1.44	94.	6.	8.90	0.2
Fused quartz	0.2-4.5	1.46	94.	18.	1.75	Insoluble
Glass	0.3-2.7	1.51-1.90	82.*-92.	200.	1.00-25.00	Insoluble
Sapphire	0.2-6.5	1.70	88.*	5.	15.00	Insoluble
Arsenic trisulfide glass	1.0-12.	2.40	75.*	18.	22.50	Insoluble
Silicon	1.2-15.	3.44	54.*	12.	7.95	Insoluble
Germanium	1.8-22.	4.03	47.*	20.	7.95	Insoluble
Cesium iodide	0.25-70.	1.7	86.	6.	12.45	44.
Indium arsenide	3.8-7.	3.5	53.*	3.	71.00	Insoluble
KRS-5	0.5-40.	2.35	72.	4.	16.00	0.05
Sodium chloride	0.2-26.	1.52	92.	12.	0.75	35.7
Sodium fluoride	0.2-15.	1.30	96.	3.	8.90	4.22
Potassium bromide	0.2-40.	1.53	92.	12.	1.35	53.5
Potassium chloride	0.2-30.	1.5	93.	12.	3.55	34.7
Potassium iodide	0.4-42.	1.60	89.	8.	3.55	140.

* Can be antireflection coated so that transmittance is greater than 95 percent.

Sources: "State-of-the-Art Report Optical Materials for Infrared Instrumentation," University of Michigan Willow Willow Run Laboratories, January 1957.

Tech Bits, Eastman Kodak Publication for Scientists and Engineers, 1966, No. 2, pp. 11, 12, 13.

Herron Optical Company, private communication

Harshaw Chemical Company, private communication

MIL Handbook 141

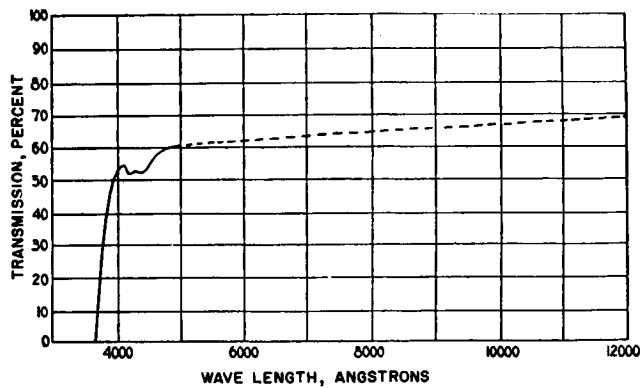


Figure A. Transmission Curve of the Lick 36-Inch Refractor and its Photographic Correcting Lens

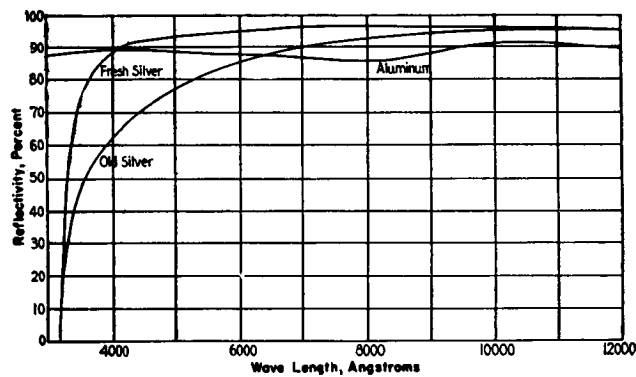


Figure B. Reflectivity of Evaporated Aluminum and Chemically Deposited Silver

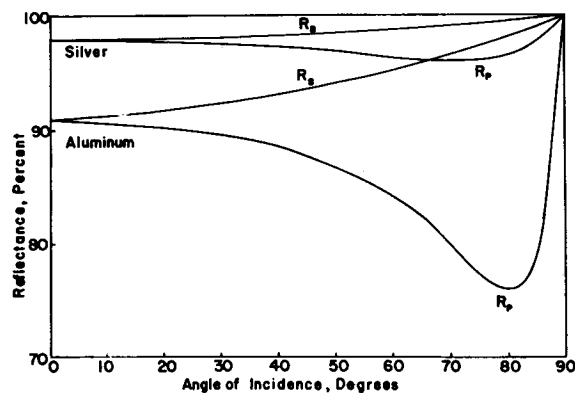


Figure C. The Reflectances of Aluminum and Silver for Different Angles of Incidence, When the Plane of Polarization is Parallel (R_p) and Perpendicular (R_s) to the Plane of Incidence

TRANSMITTING AND RECEIVING APERTURES

Optical Apertures — Optical Configurations

	Page
Effect of Surface Tolerances	296
Alignment Tolerances	298
Speed of Optical Configuration	310
Thermal Effects on Optical Configurations	312
Low Temperature Coefficient Material, CER-VIT	314

EFFECT OF SURFACE TOLERANCES

Surface tolerances must be reduced to a small fraction of a wavelength to maintain maximum energy density in the optical beam.

The accuracy of the optical system, i. e. , the optical surfaces and alignment, must be quite good to keep beam spread to a minimum. Using the perfect optical system as a reference, the loss of energy due to wave front errors can be calculated based on the work of Marechal and Francon*. The correlation between reduction in energy and wave front errors as calculated by this method is given in the Table. From these values, the need for keeping errors to a minimum can readily be seen.

Optical tolerances can be expressed in terms of the root-mean-square wave front error. The wavefront error is a combination of errors due to mirror surface errors, glass inhomogeneities, misalignment of elements and defocussing. (Discussion of alignment tolerances is given in the next topic.)

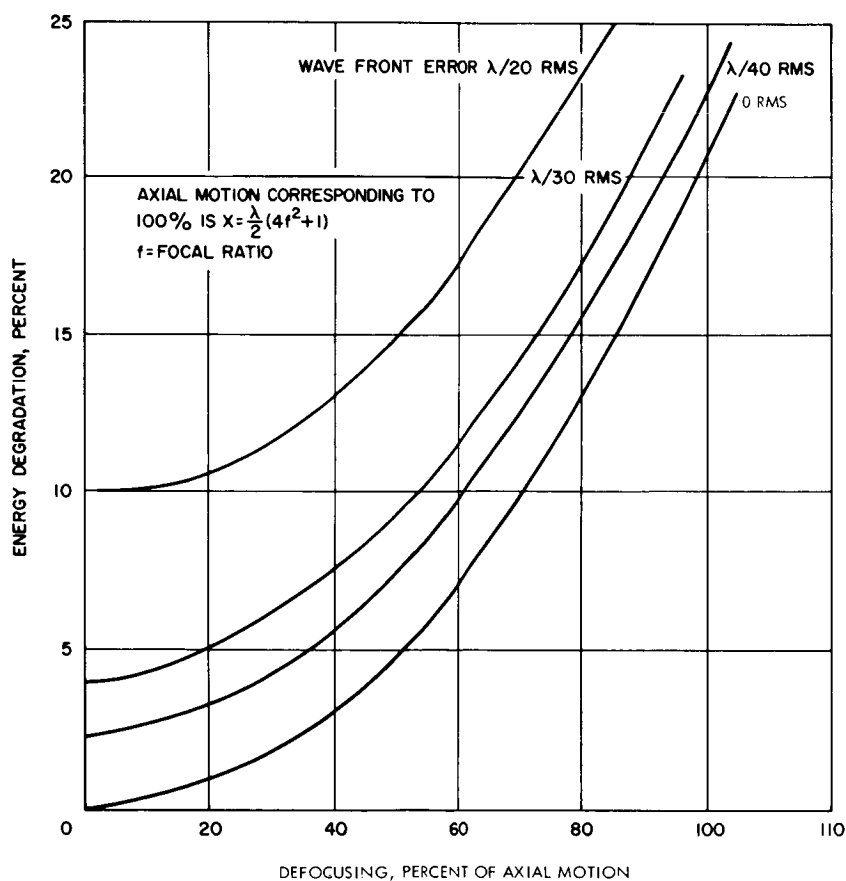
The addition of errors expressed in RMS form is not strictly correct although wave front errors along any path are additive (and can cancel each other). The figure** shows how focussing error combines with a random wavefront error to reduce contrast in a receiver or energy level in a transmitter.

* Marchal, A. and Francon, M. , Diffraction, Edit. Rv. d'Optique, Paris, 1960.

** Based on unpublished calculations by Dr. J. Kiewiet de Jonge, Allegheny Observatory and American Optical Company.

Effect of Wave Front Errors in Energy Density
at the Center of the Beam

Wave Front Errors RMS Values	Percent Reduction of Energy Density at the Center of the Beam
0	0%
$\lambda/28$	5%
$\lambda/20$	10%
$\lambda/16$	15%
$\lambda/14$	20%



Combined Defocussing and Wave Front Errors

ALIGNMENT TOLERANCES

Several alignment tolerances are given as a function of system magnification, wavelength and f-number. These tolerances are also plotted.

In general, the alignment tolerances on elements of a telescope are determined by their function in the system and the wave length of light. Thus, as the size of a telescope is increased, the tolerances do not scale and maintaining alignment becomes more difficult.

The order of magnitude of these tolerances can be seen from the following tolerance relationships for Cassegrain telescopes. All positions are relative to the primary mirror. The tolerances are:

1. Axial position of the secondary mirror

$$\Delta_{\max} = \frac{\lambda}{2} \left[4 \left(\frac{f}{m} \right)^2 + 1 \right] \quad (1)$$

based on the criterion – wavefront error not to exceed $\lambda/4$.
This equation is plotted in Figures A and B.

2. Decentration of secondary mirror

$$\delta_{\max} = \frac{13 f^3 \lambda}{m^2 - m} \quad (2)$$

based on a comatic image not to exceed Airy Disc Diameter.
This equation is plotted in Figures C and D.

3. Tilt of secondary mirror

$$\psi_{\max} = \frac{13 f^3 \lambda}{B (m^3 - m)} \quad (3)$$

based on a "comatic" image – not to exceed airy disc diameter.
This equation is plotted in Figures E and F as $(B) (\psi_{\max})$. The dimension B is defined by Figure G.

4. Position of focal plane

$$\Delta C_{\max} = \frac{\lambda}{2} (4 f^2 + 1) \quad (4)$$

based on the criterion that wavefront error is not to exceed $\lambda/4$. This equation is plotted in Figure H.

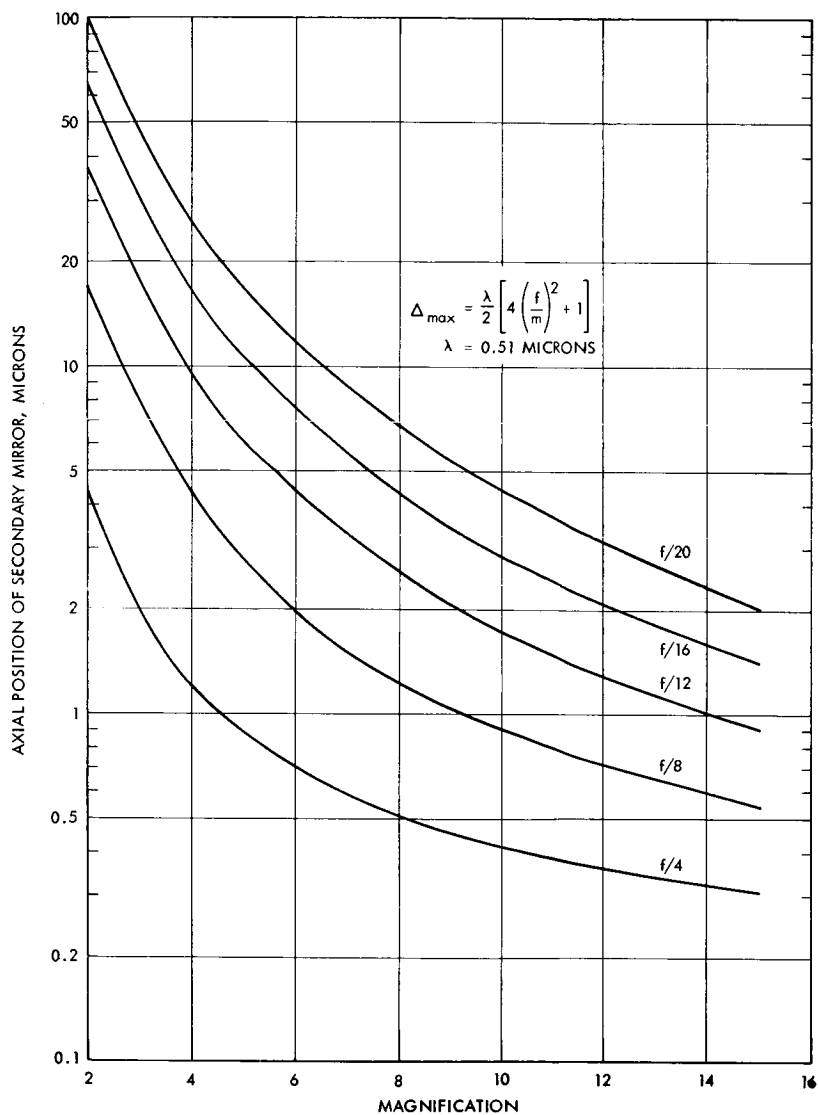


Figure A. Tolerance for Axial Position of Secondary Mirror for a Cassegrain Telescope

ALIGNMENT TOLERANCES

Symbols are defined as:

λ = wave length

f = focal ratio of Cassegrain system

m = magnification of secondary mirror of the Cassegrain system =
 C/B

A, B and C are shown in Figure G.

The tolerance budget of a system must be realistic to allow the designer to have maximum freedom possible. As an example, the equations just presented for a Cassegrain telescope tacitly assume that the focus is maintained by the control of dimensions A and C. If the focus were maintained by observation of the image in the focal plane (by an observer or automatic focusing device), then the half range of axial position of the secondary mirror, without introducing wave front errors exceeding one quarter wave, becomes

$$x_h = \frac{256 \lambda f^4}{m^5 - m^4 - m^3 + 1} \quad (5)$$

This provides considerable relaxation of this tolerance, and makes use of an optical focusing device very desirable. This equation is plotted in Figures I and J. These figures may be compared with Figures A and B to note the relaxation in tolerances.

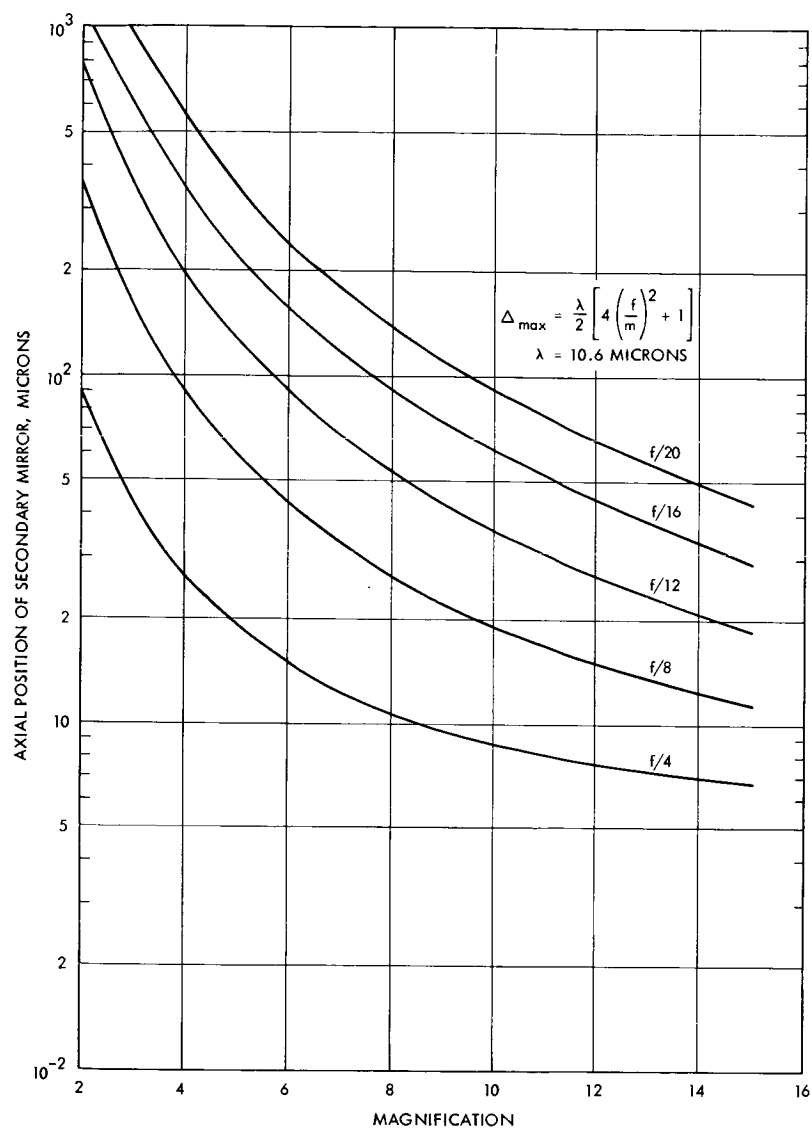


Figure B. Tolerance for Axial Position of Secondary Mirror for a Cassegrain Telescope

ALIGNMENT TOLERANCES

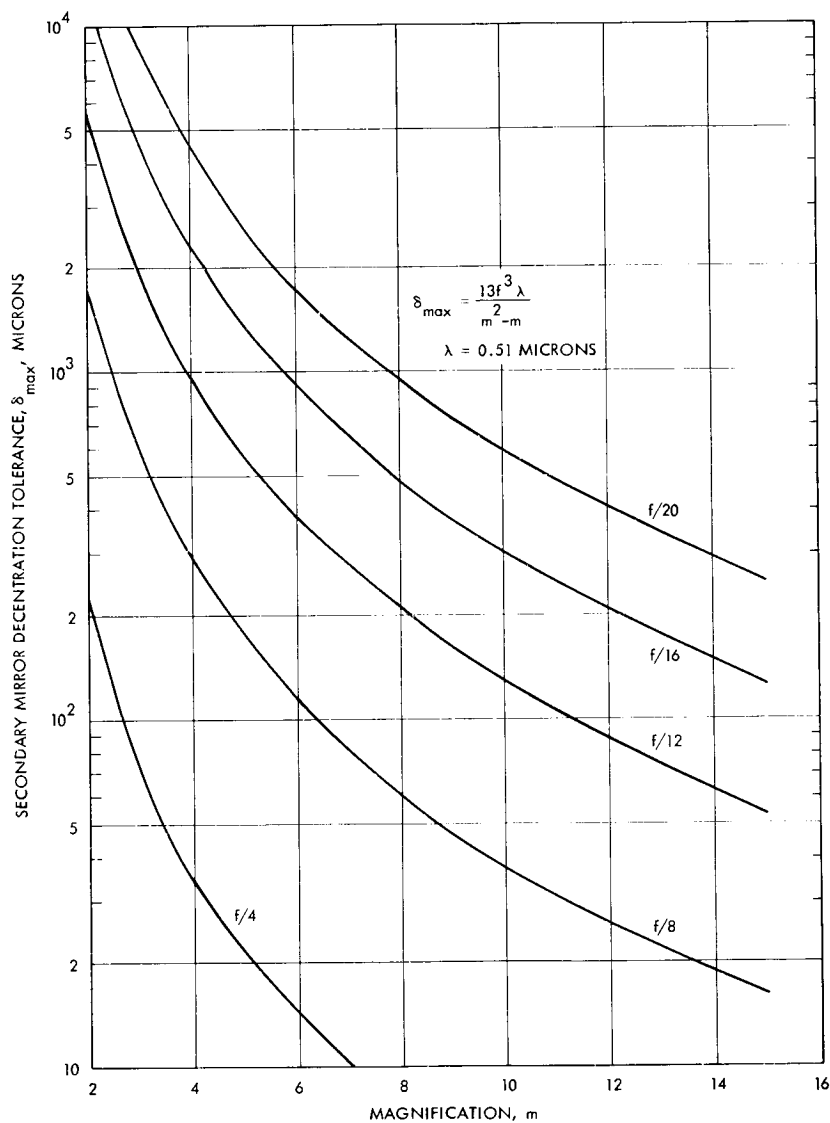


Figure C. Tolerance for Decentration of Secondary Mirror for a Cassegrain Telescope

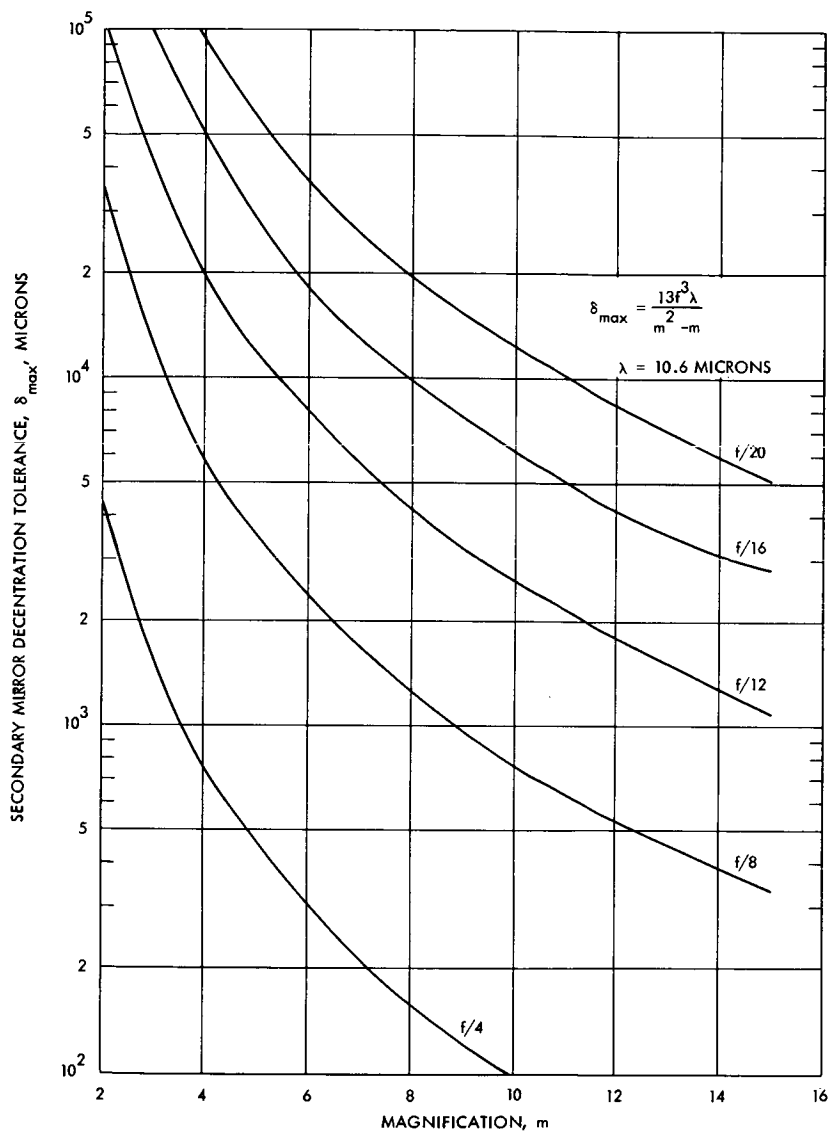


Figure D. Tolerance for Decentration of Secondary Mirror for a Cassegrain Telescope

ALIGNMENT TOLERANCES

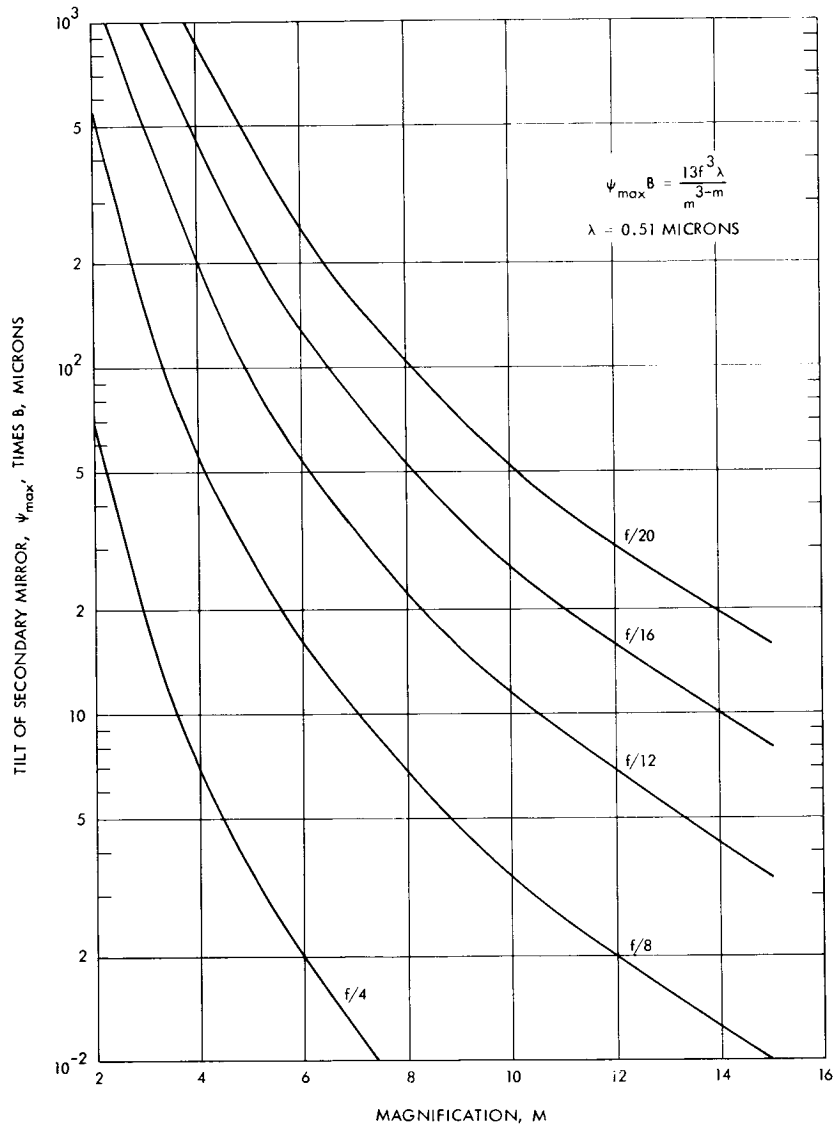


Figure E. Tolerance for Tilt of Secondary Mirror for a Cassegrain Telescope

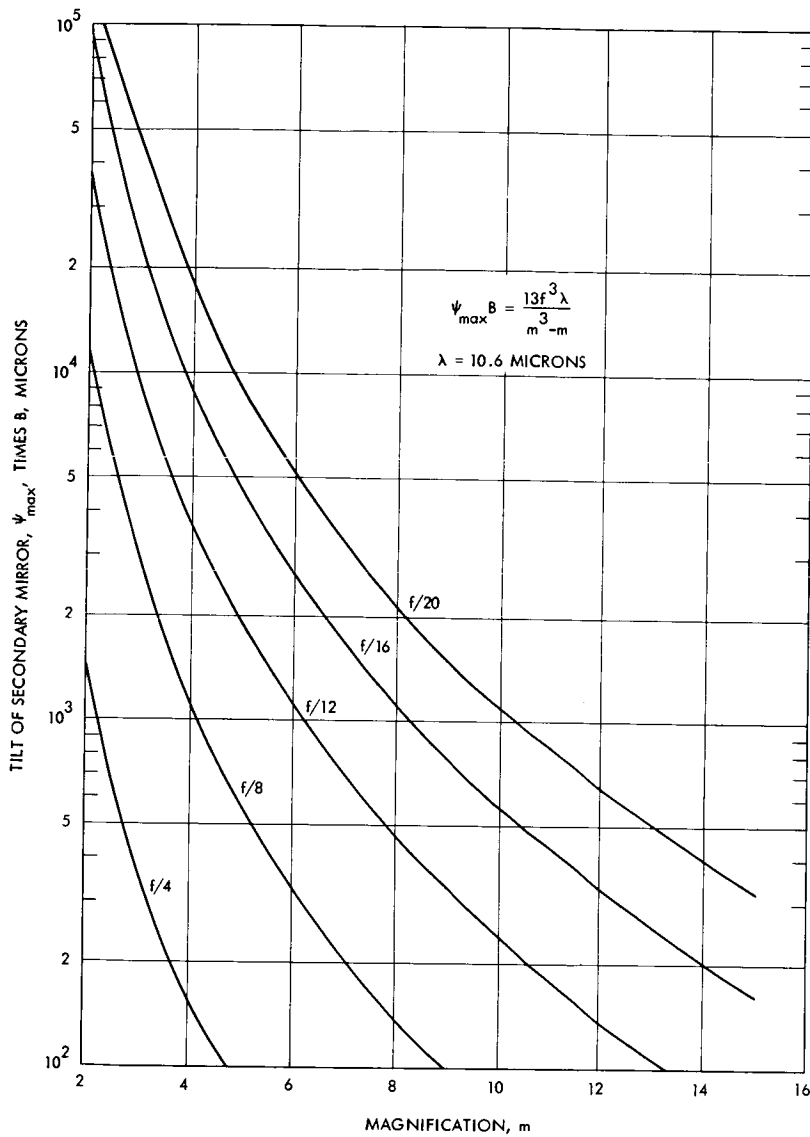


Figure F. Tolerance for Tilt of Secondary Mirror for a Cassegrain Telescope

ALIGNMENT TOLERANCES

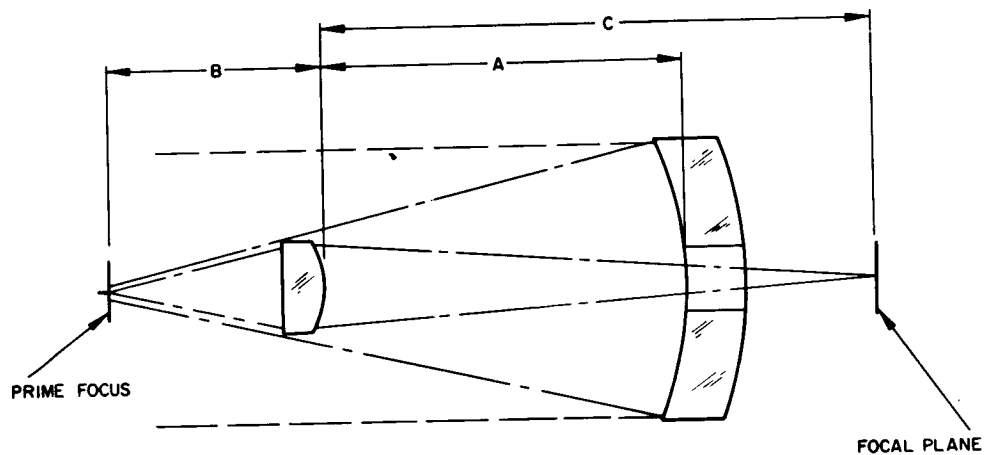


Figure G. Components of a Cassegrain System

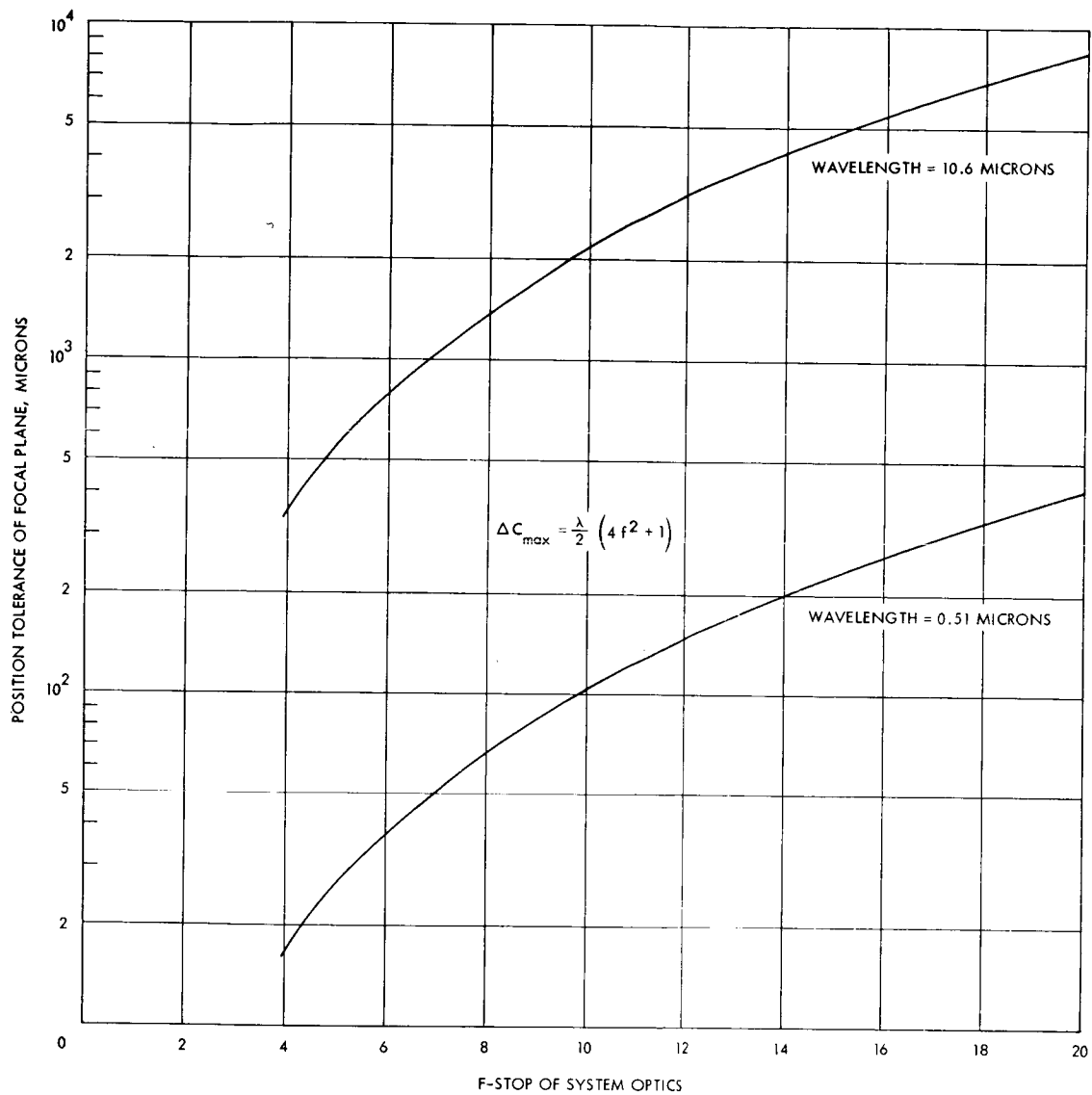


Figure H. Tolerance on Position of Focal Plane for a Cassegrain Telescope

ALIGNMENT TOLERANCES

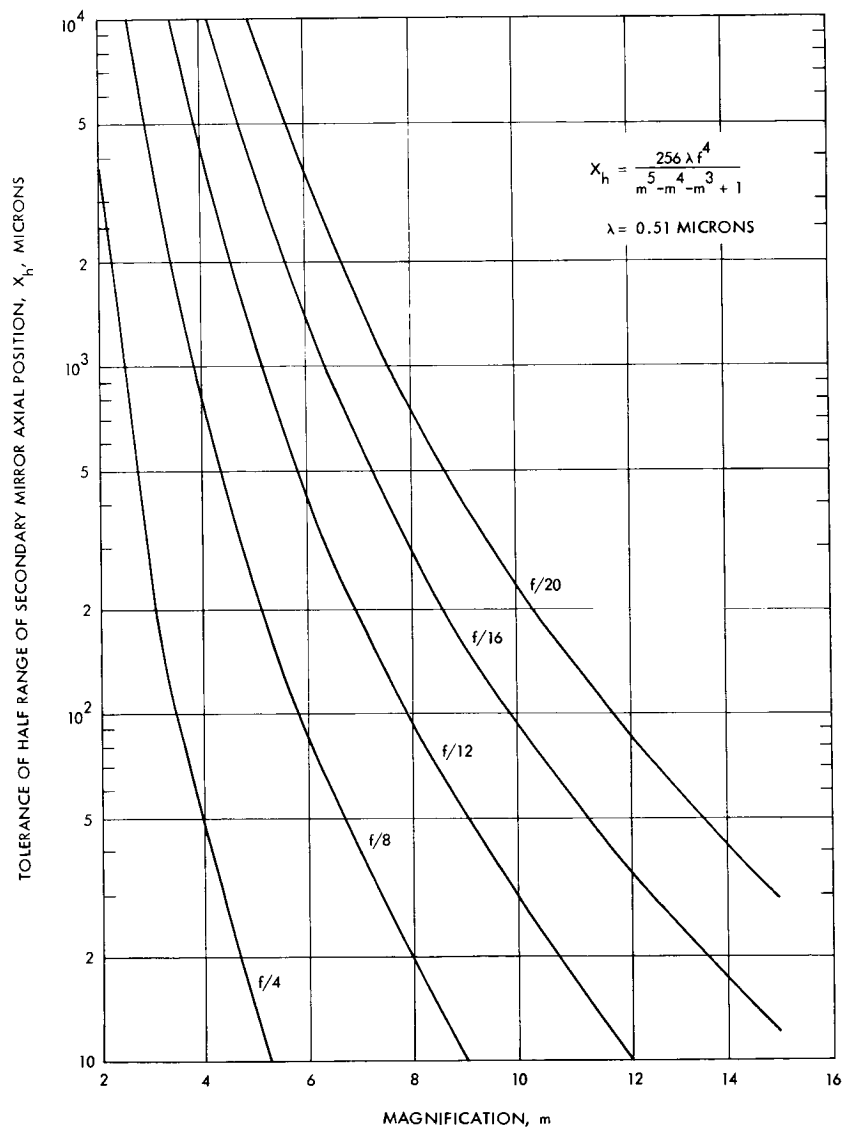


Figure I. Half Range of the Secondary Mirror Axial Position for a Cassegrain Telescope

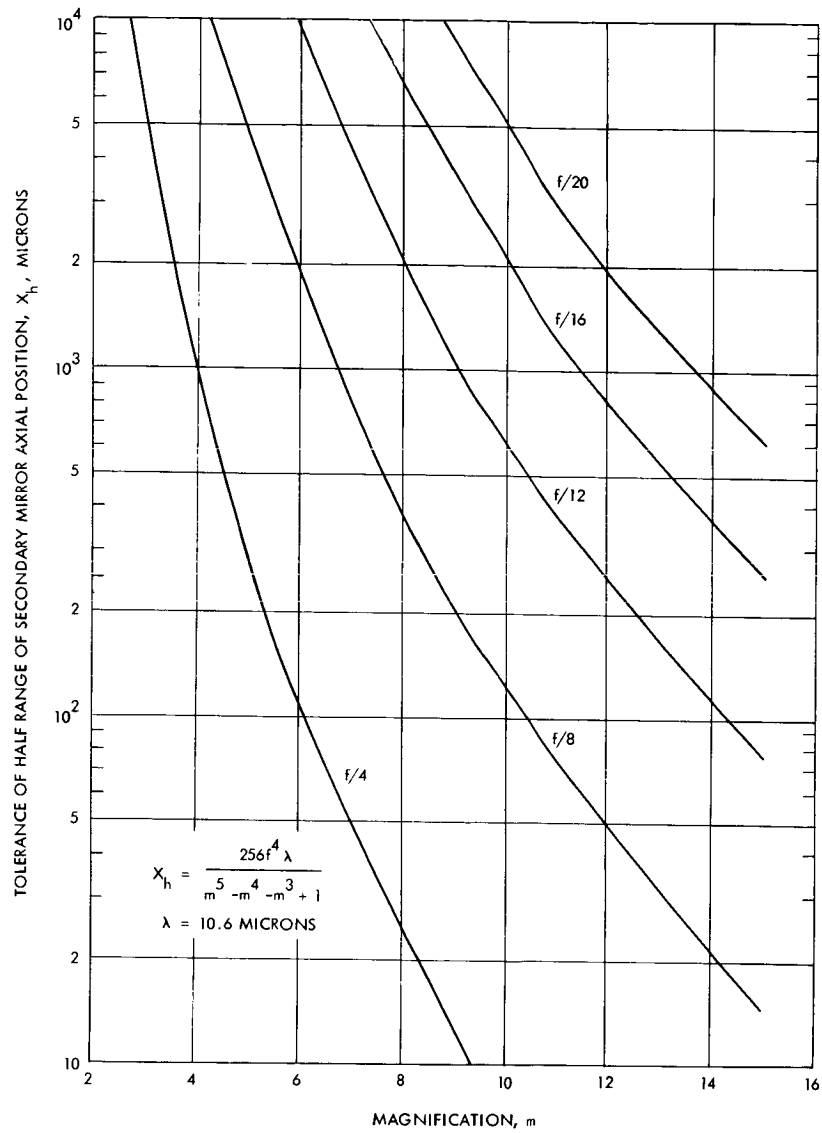


Figure J. Half Range of the Secondary Mirror Axial Position for a Cassegrain Telescope

SPEED OF OPTICAL CONFIGURATION

Higher speed optics (low f-number) are desirable for space configurations from the point of view of inertia, weight, rigidity and cost.

For a high performance spaceborn optical system, the addition of any weight to the system adds greatly to the cost. Thus, first consideration is given to lightweight optical mirror design which may have large apertures, and systems which can be built around such mirrors.

In a reflecting system, the primary mirror focal ratio of "speed" is one of the more difficult parameters to evaluate clearly since there are several trade-offs that must be made simultaneously. As far as optical manufacturability is concerned, it is easier to make a "slow" (large f-stop or ratio of focal length to diameter) paraboloid by the conventional optical processes. As the speed of a paraboloid is increased, the deviation from spherical becomes greater and optical manufacturing difficulties increase very rapidly. Testing also increases in difficulty with very "fast" (shorter focal length) mirrors. But the overall performance penalties for using a slow primary are severe. The system becomes much longer, has greater weight and inertia and is harder to hold rigid. There are also difficulties in obtaining large field coverage without excessive obscuration. Some of the same types of tradeoffs affect the design of conventional astronomical telescopes, since the use of a slow primary increases the size and weight of the telescope and dome. It is fairly well established that faster the primary mirror, the lower the overall cost of an astronomical telescope despite the increased time required to figure the primary mirror.

Under the pressure of these factors, there have been some recent improvements in the techniques of making and testing large aspherics and additional work is continuing. Probably the most significant technique makes use of an extremely accurate turntable to generate an aspheric curve with an absolute minimum of astigmatism. This allows the manufacture of faster, higher quality mirrors than were heretofore possible. Thus, large mirrors (approximately 1 meter) of $f/2$ or $f/1.5$ are now quite feasible.

THERMAL EFFECTS ON OPTICAL CONFIGURATIONS

Lateral and front to back thermal gradients are considered for the primary mirror of an optical system and a means for accommodating temperature effects is suggested.

A critical area in the design of a large optical systems for space use is that of thermal control. The effect of variations in temperature, with non-uniformity in temperature distribution, will be to distort the optical system. Both the structure and the elements themselves will be distorted. However, an automatic alignment system can be provided to compensate for the effects on the structure. Thus, it is the effect on the largest element (the primary mirror) that is of greatest concern.

The effects of a change in average temperature on a large lightweight mirror have not been determined. If the effect was a uniform expansion, there would be no change other than a change of the focal length. However, the actual mirrors are not perfectly uniform. For instance, beryllium sandwich mirrors are coated with nickel that has an expansion coefficient close to but not identical with that of beryllium. This produces a bi-metal effect if the nickel is not of the same thickness on front and back. Even fused silica sandwich mirrors have some impurity content and slight devitrification that would cause distortion with a change in ambient temperature.

The effects of non-uniformities in temperature can pose an extremely complex problem unless some simplifying assumptions are made. The assumption will be made that the temperature distribution in primary mirror can be approximated by linear gradients. The practical necessity of thermally isolating the mirror will result in any change taking place slowly and will result in the actual temperature distribution being reasonably close to linear.

A linear front-to-back gradient will cause a bending of the mirror such that the change in focal length, ΔF , will be given by:

$$\Delta F = \frac{2F^2 n \Delta T}{t}$$

where

F = focal length

n = coefficient of expansion

ΔT = temperature difference, front to back of mirror

t = thickness of the mirror

The first order effect can be removed by focussing, but the accompanying higher order effects will determine the actual limit of permissible gradient. This gradient is controlled both by the thermal isolation (with control of shielding temperatures) and by changing the effective

cross-sectional area of the core of the sandwich mirror to provide sufficient area for conduction. In this regard, if a large cross-sectional area is required, there is a heavy weight penalty.

Control of lateral gradients in the mirror will require careful design of thermal shields. A linear lateral temperature gradient results in wavefront distortion given by:

$$\delta = \frac{n \Delta T D^2}{16 F}$$

where

δ is the total wavefront distortion

n is the coefficient of expansion of the mirror material

D is the diameter of the mirror

F is the focal length of the mirror

ΔT is the difference in temperature, edge to edge along the meridian in the direction of the gradient

The curvature of the mirror varies with the position along the meridian in the direction of the gradient. The result is an elongated image in this direction. Applying this equation and a quarter wave distortion limit to large mirrors of reasonable focal lengths, results in a rather small temperature gradient tolerance; particularly for beryllium mirrors. However, beryllium, because of its high thermal conductivity, will handle a greater heat flow without exceeding the tolerance than will fused silica. Beryllium also has a peculiar property at cryogenic temperatures that is most valuable. Below 70°K the coefficient of expansion is essentially zero.

Two causes for thermal gradients in the mirror are the heat within the surrounding structure and the differences in radiation to the various parts of the front face from the exterior. Both can be controlled by shielding, although the latter source is less controllable.

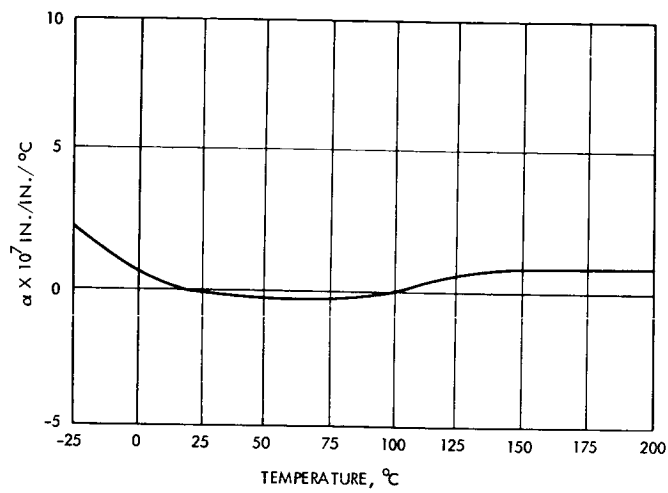
Many optical systems have been built to accommodate variations in ambient temperature. Some very ingenious mechanisms have been tried, often employing invar (low expansion) rods. However, a very simple solution is often possible. In this simple method a passive means of compensation is employed. If the optical system and supporting structure can all be made of materials having the same or nearly equal coefficients of expansion, then the optical system will only change in scale. That is, the image plane will always remain in focus but with a slightly different magnification or equivalent focal length. Beryllium optical components can often be supported by a beryllium structure to achieve this result. Care should be taken to design around beryllium's notch sensitivity. Glass components can be supported by titanium or 400 series stainless steels to achieve the same effect. Fused silica or Cer-Vit (see next topic) components would require an invar flotation system to accomplish the same result.

LOW TEMPERATURE COEFFICIENT MATERIAL, CER-VIT

Cer-Vit has a very low temperature coefficient which makes it a candidate material for spaceborn optical apertures.

Cer-Vit, similar to fused silica, has a peculiar coefficient of thermal expansion. It varies, but does not exceed $2 \times 10^{-7}/^{\circ}\text{C}$ over the range $0 - 300^{\circ}\text{C}$. The null points of the expansion coefficient curve can be shifted back and forth in the initial processing to a marked degree. A typical expansion curve is shown in the Figure.

Owens-Illinois have made mirror blanks of Cer-Vit up to 41 inches diameter to date. Segmented mirrors from 60 to 72 inches have been made. Cer-Vit is melted and formed as a glass, then by treatment is converted to a partially crystalline body. The most valuable property of Cer-Vit is its low coefficient of expansion - adjustable over a wide temperature region. It can be cored by casting or by subsequent grind-out. Present cost of a six-inch diameter blank one inch thick is \$65.00. Cer-Vit will also transmit to 4 microns for infrared uses, but exhibits some back scatter. It is both harder and stiffer than fused silica but has slightly less thermal shock tolerance and a lower maximum service temperature.



A Typical Expansivity Curve for Low Expansion Cer-Vit Mirror Material

TRANSMITTING AND RECEIVING APERTURES

Optical Frequency Apertures – Weight and Cost Relationships

	Page
Weight and Cost of Beryllium Mirrors	318
Weight and Cost for Fused Silica Mirrors	322
Weight and Cost Burden Relationships	324

WEIGHT AND COST OF BERYLLIUM MIRRORS

Weight and cost estimates are given for beryllium mirrors and for mirrors plus structure as a function of mirror aperture.

Mirrors Weight and Cost

Beryllium mirrors of high quality have been made in sizes up to 24 inches. Larger sizes have been made with lower quality. At present, there is no reason to believe that there is any basic size limitation for properly designed, high quality beryllium mirrors. The present beryllium pressing capacity limits sizes to about 7-feet in diameter without additional expenditures for facilities.

A cored center, sandwich construction, for beryllium mirrors is sometimes used to save weight and retain a very high bending stiffness. High bending stiffness helps resist bimetal bending caused by differential thermal expansion of the beryllium and the electroless nickel coating that is applied to these mirrors to provide a polishable surface. This effect can be minimized by coating both sides of the blank. The high bending stiffness also helps in resisting the vibration environment of the rocket launch.

An approximate curve relating beryllium mirror weight to aperture is included as Figure A, based on sandwich construction of reasonable proportions. A curve giving the approximate cost of beryllium mirrors is shown in Figure B.

Mounted Mirrors Weight and Cost

The primary mirror cell weight depends strongly on its orientation during launch relative to the steady acceleration and shock loads. Beryllium mirrors would require less weight for launch support than fused silica, making the total weight saving using a beryllium mirror considerably greater than the savings of the blank weight alone.

The weight range for the mechanical and optical structure of the telescope proper is shown in Figure C. These are for a telescope using beryllium optical components given as a function of aperture.

The cost range for the mechanical and optical structure of the telescope proper is shown in Figure D. These costs are for a telescope using beryllium optical components as a function of aperture.

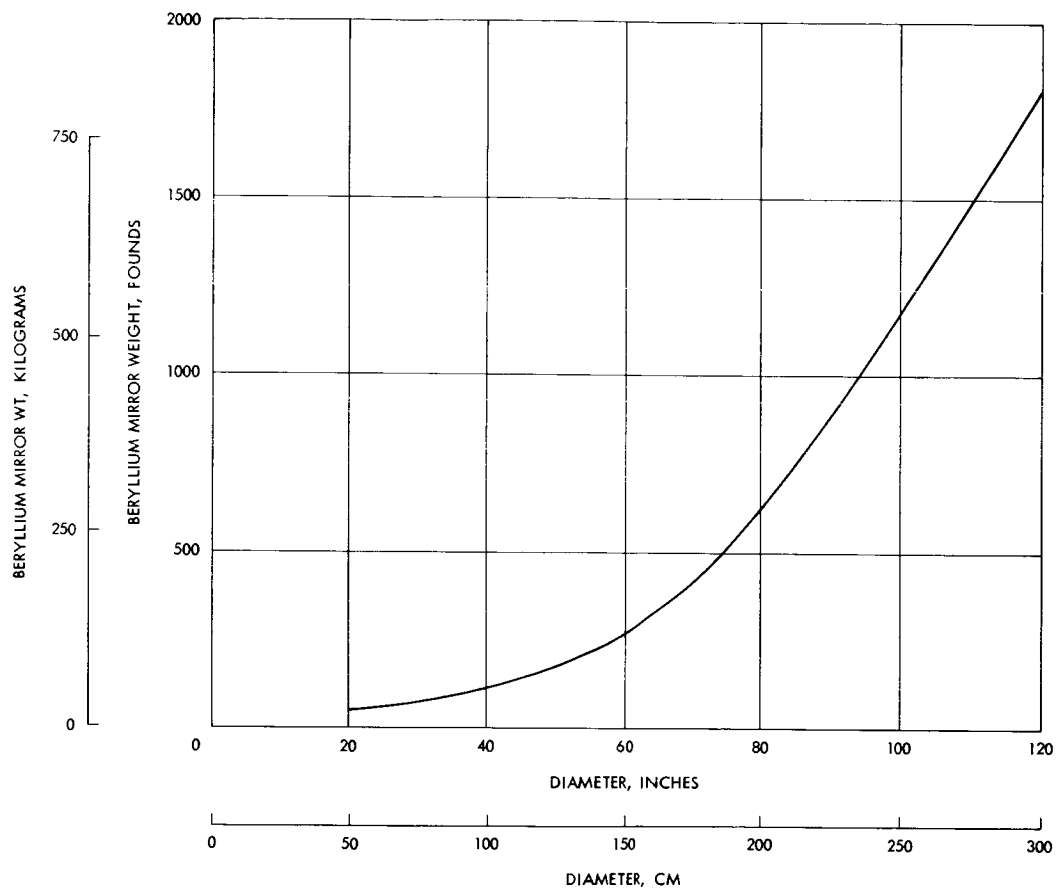


Figure A. Approximate Mirror Weight of Beryllium Sandwich Mirrors

WEIGHT AND COST OF BERYLLIUM MIRRORS

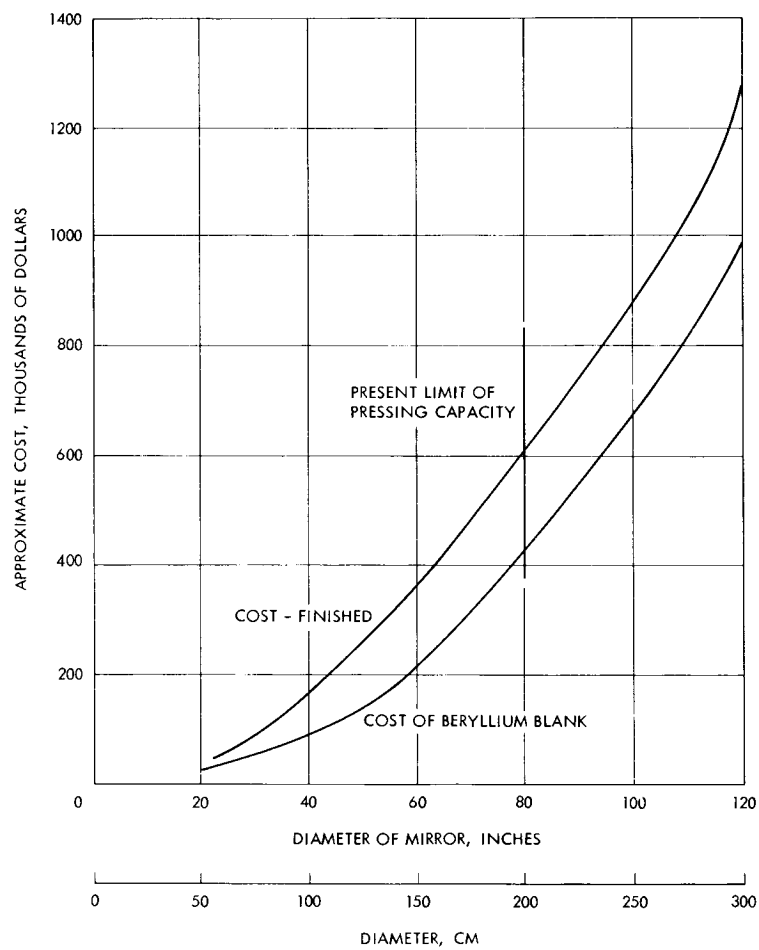


Figure B. Approximate Cost of Beryllium Sandwich Mirrors

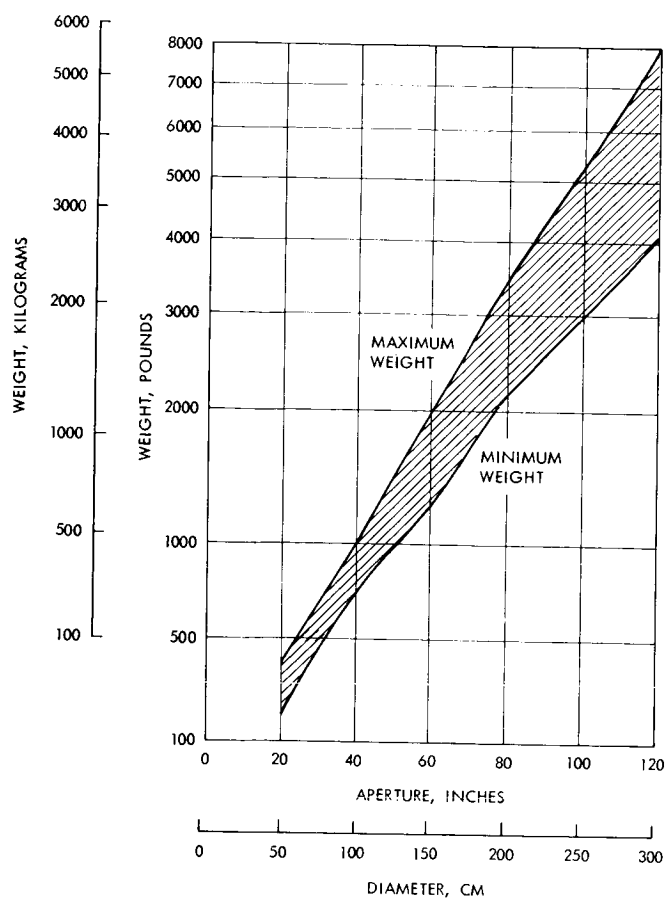
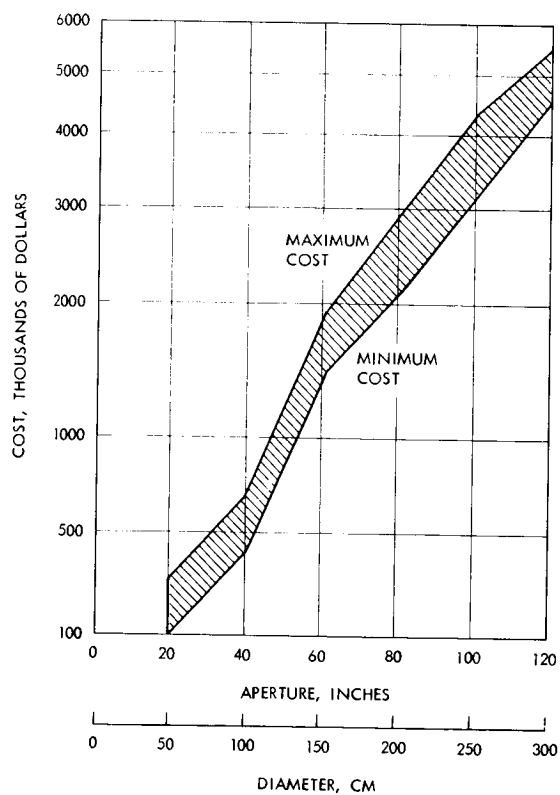


Figure C. Preliminary Weight Estimate for the Telescope Mechanical and Optical Structure Using Beryllium Optical Components

Figure D. Preliminary Cost Estimate for Mechanical and Optical Structure Using Beryllium Optical Components



WEIGHT AND COST FOR FUSED SILICA MIRRORS

Weight and cost estimates are given for lightweight, cored center silica mirrors.

Corning Glass Works have made lightweight, cored center, sandwich type, fused silica mirror blanks in sizes up to about 45 inches in diameter. Their present capacity to make bowls of fused silica limits them to about 80-inch sizes without making face plates by fusing smaller pieces together, a procedure that would require additional development work.

General Electric is developing a procedure to make lightweight blanks that would involve cutting the face plates and center core from solid blocks. These are made by fusing many hexagonal ingots together.

The approximate weights of fused silica mirror blanks are plotted against size in Figure A for normal proportions. A similar curve giving the approximate cost of fused silica mirrors is shown in Figure B.

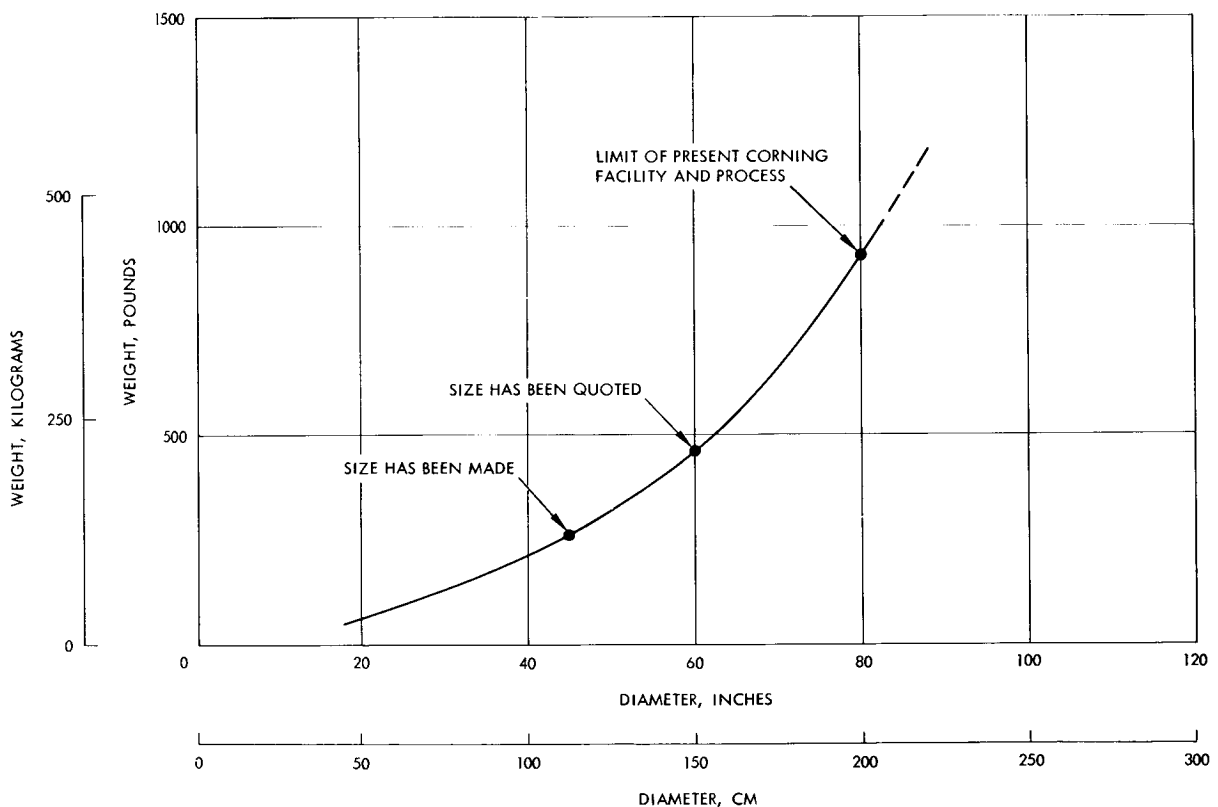


Figure A. Approximate Mirror Weight of Fused Silica Sandwich Mirrors

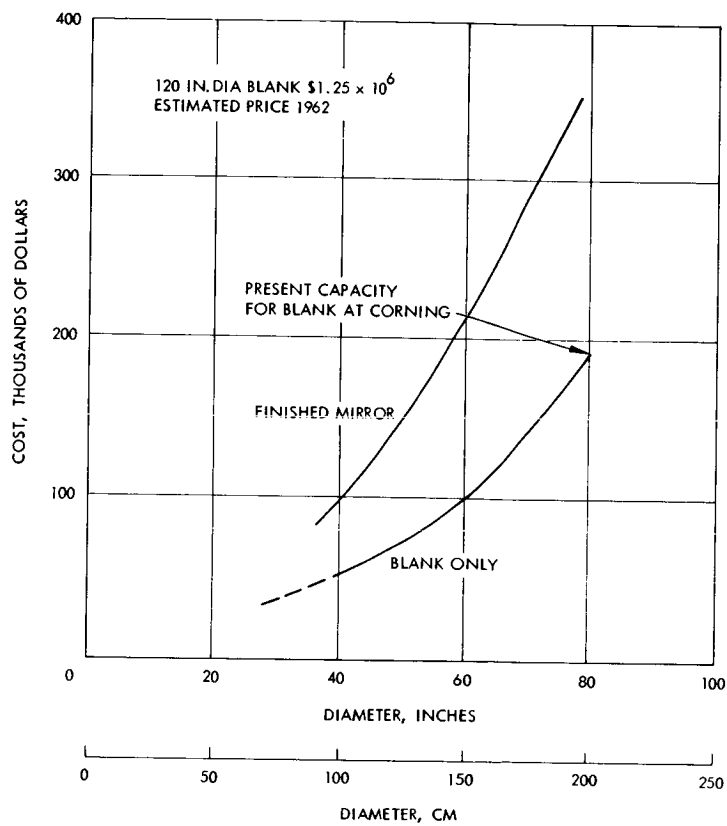


Figure B. Approximate Cost of Fused Silica Sandwich Mirrors

WEIGHT AND COST BURDEN RELATIONSHIPS

The relationships between weight and aperture diameter and cost and aperture diameter are modeled in a form suitable for the Communications System methodology.

The previous two topics gave estimate bounds for the cost and weight of optical assemblies as a function of aperture diameter. These may be modeled using the cost and weight models of the communications system methodology discussed in Volume II of this final report. The model used for weight and cost are as follows. The weight of the transmitting aperture is given by the relationship

$$W_{d_T} = K_{d_T} (d_T)^{n_T} + W_{KT} \quad (1)$$

where

d_T = the transmitting aperture diameter

K_{d_T} = a constant relating transmitting antenna weight to transmitting aperture diameter

W_{KT} = transmitting antenna weight independent of transmitter aperture diameter

n_T = a constant

and the aperture cost is given by

$$C_{\theta_T} = K_{\theta_T} (d_T)^{m_T} + C_{KT} \quad (2)$$

where

K_{θ_T} = constant relating transmitter antenna fabrication cost to transmitter aperture diameter

m_T = a constant

d_T = transmitting antenna diameter

C_{KT} = transmitter antenna fabrication cost independent of transmitter diameter

Equation 1 and 2 refer to the transmitting aperture cost and weight. These can be made to refer to the receiver cost and weight by replacing the "T" in the subscripts with "R".

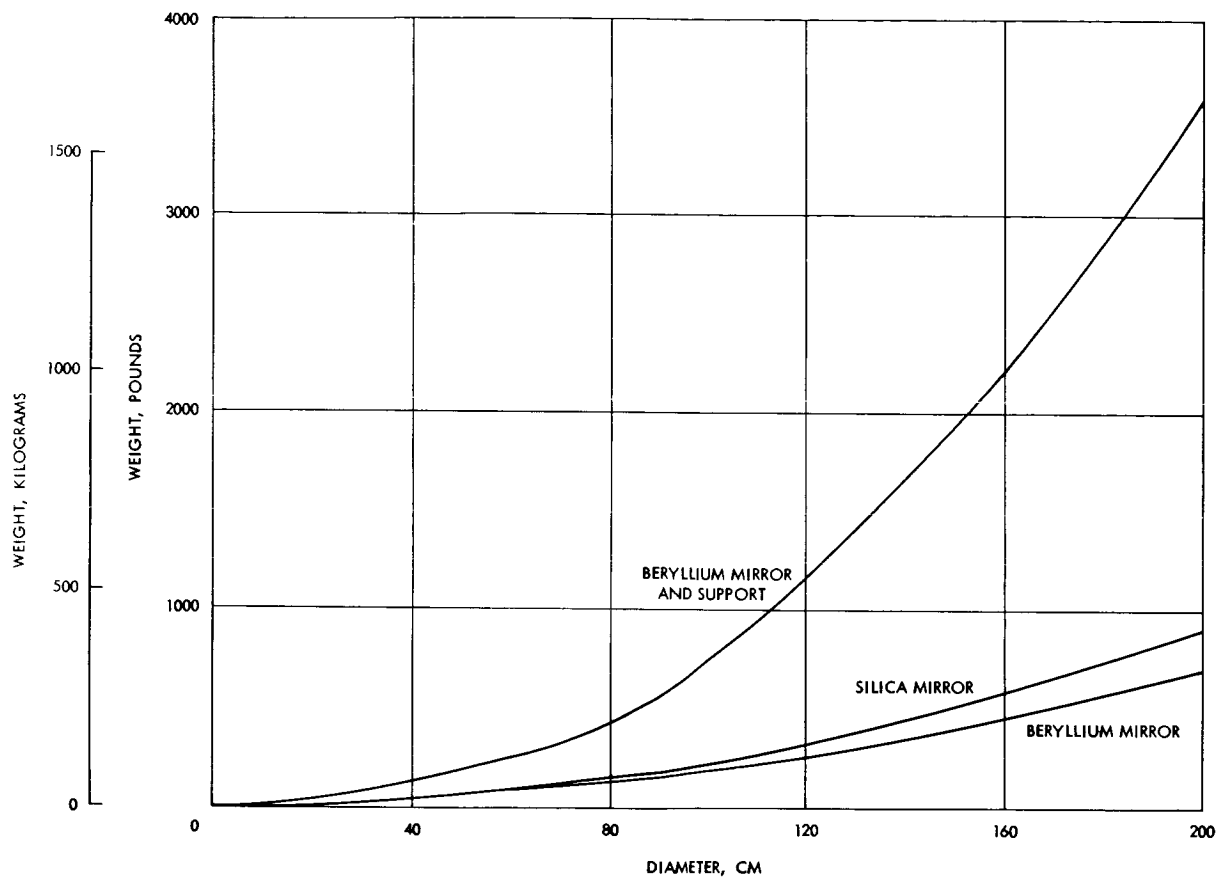


Figure A. Weight Burden Relationships for Optical Apertures

Transmitting and Receiving Apertures
Optical Frequency Apertures – Weight and Cost Relationships

WEIGHT AND COST BURDEN RELATIONSHIPS

The values for the burden constants, based on the previous two topics, are given in Tables A and B. Equations (1) and (2) are then plotted in Figures A and B.

Table A. Weight Burdens for Optical Apertures

Burden Constant	Mirror Only		Mirror and Support Structure
	Beryllium	Silica	Beryllium
W_{KT}, W_{KR}	5	10	25
K_{dT}, K_{dR}	0.0057	0.0074	0.0303
n_T, n_R	2.2	2.2	2.2

Table B. Cost Burdens for Optical Apertures

Burden Constant	Mirror Only		Mirror and Support Structure
	Beryllium	Silica	Beryllium
C_{KT}, C_{KR}	25,000	20,000	40,000
$K_{\theta T}, K_{\theta R}$	15	8.75	72
m_T, m_R	2	2	2

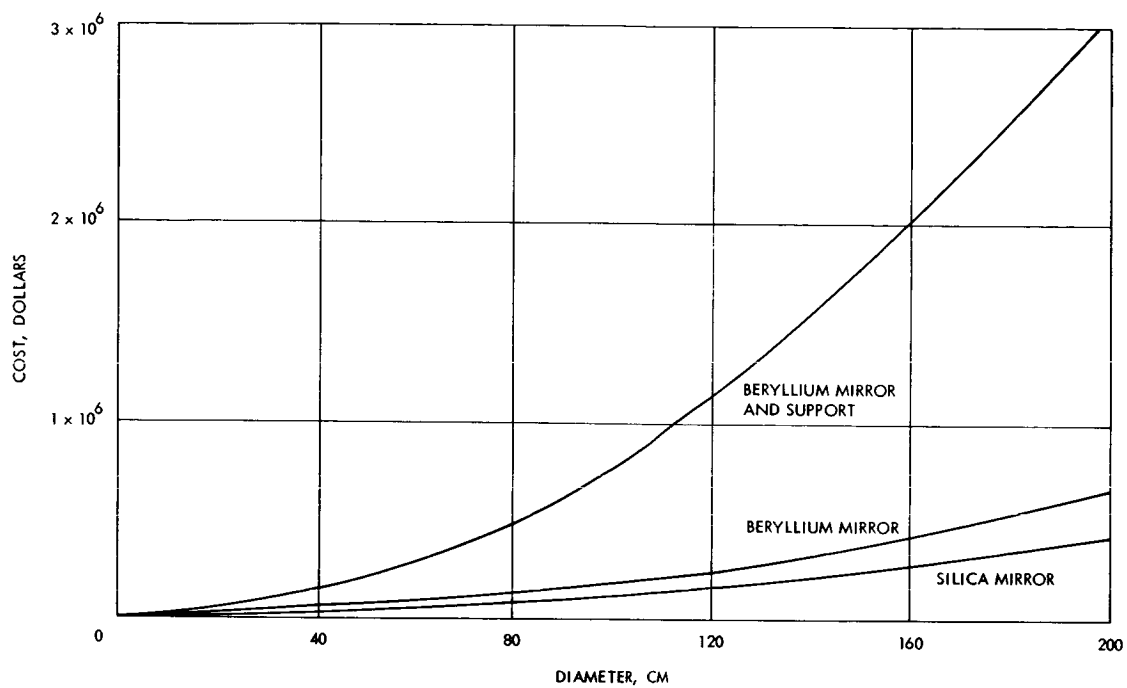


Figure B. Cost Burden Relationships for Optical Apertures

PART 5 – ACQUISITION AND TRACKING

Section	Page
GENERAL ACQUISITION AND TRACKING SYSTEM CONSIDERATIONS	334
Mission Associated Considerations	334
Receiver Location Considerations	346
ACQUISITION AND TRACKING SYSTEM PERFORMANCE ANALYSIS	353
The Tracking Subsystem – Introduction	358
Acquisition	380
Detection Theory	386
Angle Noise Error in Optical Tracking Systems	396
COMPONENT PERFORMANCE AND BURDEN RELATIONSHIPS	424
Attitude and Tracking Sensors	424
Attitude Control Techniques	440
Passive Attitude Control Techniques	444
Active Attitude Control Devices	452
Burden Relationships	466